WIDE AREA MONITORING SYSTEM

A DISSERTATION

submitted by

Ravi Kumar Singh

Enrolment No: 16529015

Under the guidance of

DR. PREMALATA JENA

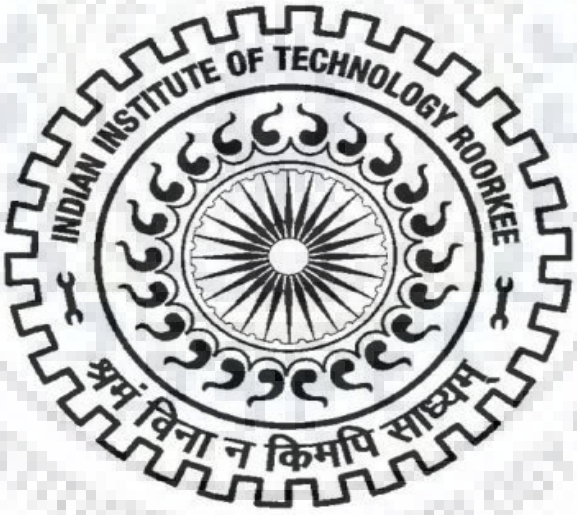

DEPARTMENT OF ELECTRICAL ENGINEERING
INDIAN INSTITUTE OF TECHNOLOGY ROORKEE
ROORKEE – 247667 (INDIA)

CANDIDATE'S DECLARATION

I hereby declare that this dissertation entitled WIDE AREA MONITORING SYSTEM which is being submitted to the Department of Electrical Engineering, Indian Institute of Technology, Roorkee in fulfillment of the requirements for the award of the Degree of Master of Technology in Electrical Engineering with specialisation in Power System Engineering is a bonafide work carried out by me during the period May 2017 to May 2019 under the supervision of Dr. Premalata Jena, Assistant Professor, Department of Electrical Engineering, IIT Roorkee. The material contained in this dissertation has not been submitted by me for the award of any other degree of this institute or any other institute.

Date : RAVI KUMAR SINGH

Place : Roorkee (En. No.-16529015)

CERTIFICATE

This is to certify that the above statement made by the candidate is true to the best of my knowledge and belief.

DR. PREMALATA JENA

Assistant Professor

Department of Electrical Engineering

Indian Institute of Technology Roorkee

ACKNOWLEDGEMENT

I would like to express my deepest gratitude to my guide, Dr. Premalata Jena, who gave me this opportunity to work and execute this project under his guidance and support. I am grateful to her for providing me with helpful feedback throughout the course of this work which helped me bringing this work to a successful completion. Her suggestions and guidance helped me in improving the quality of my work. Also, I wish to extend my sincere thanks and express my indebtedness to the PhD research scholars who have helped me immensely in my dissertation work.

At last, I would like to thank all those who helped me, directly or indirectly, in any part of this work which I have been able to complete in due time.

ABSTRACT

Power systems are operating in a more complicated and therefore encounter more challenges. If one part of a power grid becomes seriously out of synchronism with the rest, the whole network can become unstable and blackout may occur. In this regard, we need to use advanced and smart monitoring tools to quickly and reliably observe the changing state of the key electrical parameters in real time, take appropriate corrective measures and isolate faults.These technologies should integrates the functions of monitoring, protection and control in the power systemsystem.Phasor Measurement Units (PMUs) by employing satellite technology (GPS) , offer a state-of-the-art Wide Area Monitoring System (WAMS) for improving power system monitoring, control and protection.

In this report, we present information about WAMS components and requirements for transmission.We will discuss the concept of PMU placement, PMU simulink model, its application as fault locator and how it can be used to identify a power swing. The simulation results show that with the use of PMU we can immediately locate the position of fault and identify a power swing as stable and hence can help in sending a blocking signal to the relay to prevent its maloperation.

The simulations have been carried out in PSCAD v4.5 software and the calculations and plots have been obtained by making use of MATLAB 2014a software.

CONTENTS

CANDIDATE DECLARATION		(i)
CERTIFICATE		(i)
ACKNOWLEDGEMENT		(ii)
ABSTRACT		(iii)
LIST OF FIGURES		(vi)
1	**Introduction**	1
1.1	Wide area monitoring system	1
1.2	Architecture of WAMS	2
1.3	Benefits of WAMS	3
2	**Phasor measurement unit (PMU)**	**4**
2.1	Phasor	4
2.2	IEEE Standards for synchrophasor measurements	5
2.3	PMU installation	6
2.4	PMU hardware block diagram	7
2.5	PMU performance criteria	7
2.6	PMU challenges	8
3	**Other components of WAMS**	**9**
3.1	Phasor data concentrator	9
3.2	Communication network	10

3.3	WAMS applications for power system	11
3.4	RTDMS	11
4	**PMU Model in MATLAB/SIMULINK**	**12**
5	**PMU Data Based Fault Location**	**20**
5.1	Two ended negative sequence impedence method	20
5.2	Simulation results for different fault location for Two ended negative sequence impedence method	22
5.3	Two ended method based on distributed parameter Transmission line model	25
5.4	Simulation results for different fault location based On distributed parameter transmission line model	27
5.5	Estimation of fault location location on UHV Using PMU	31
6	**PMU application in indentifying a power swing**	**38**
6.1	Methodology	38
6.2	Determination of type of power swing	42
6.3	Simulation studies on 3 bus system	43
7	**Result And Discussion**	**44**
REFERRENCES		**45**
Appendices		**48**
Appendix A	Fault locator algorithm using PMU measurements	49
Appendix B	Parameters of transmission line used as test system for fault location	50

LIST OF FIGURES

1.1	WAMS Basic Architecture	2
2.1	Phasor representation	5
2.2	PMU connection	6
2.3	PMU hardware block diagram	7
2.4	Measurement of TVE	8
4.1	SIMULINK Block diagram of PMU	15
4.2	WAMS main simulink block diagram	16
4.3	Current magnitude measurement	17
4.4	Voltage magnitude measurement	17
4.5	Current angle magnitude measured	18
4.6	Frequency measurement	18
4.7	Rate of change of frequency	19
5.1	One line two source circuit	20
5.2	Sequence network for one two source circuit	21
5.3	SLG fault occured at sending end m = 0	23
5.4	SLG fault occured at receiving end m = 1	23
5.5	SLG fault occured at m = 1/4	24
5.6	SLG fault occured at m = 1/3	24
5.7	SLG fault occured at m = 1/2	25
5.8	One line two source circuit	25
5.9	Single phase faulted transmission line with two sources	27
5.10	Single phase fault location with D = 1	28
5.11	Single phase fault location with D = 0	39
5.12	Single phase fault location with D = 0.2	30

5.13 Transmission line under pre-fault and during fault conditions……... 31

5.14 Test system of 765 kv…….. 32

5.15 Fault current in line 3-7 for 3ph-g fault for p=0.8 for fault at 0.4sec….. 33

5.16 Current phasor for 3ph-g fault for p=0.8 using DFT (0.40sec)…… 34

5.17 Fault current in line 3-7 for 3ph-g fault for p=0.8 for fault at 0.45sec… 35

5.18 Current phasor for 3ph-g fault for p=0.8 using DFT (0.45sec……. 35

5.19 Fault current in line 3-7 for 3ph-g fault (100km from unnao)……. 36

5.20 Voltage at bus 3 for 3ph-g fault (100km from unnao)…….. 36

5.21 Fault location index p for 3ph-g fault (100km from unnao)……. 36

5.22 Fault detection index *Num* for 3ph-g fault (100km from unnao)…….. 37

5.23 Fault detection index *Num* for 3ph-g fault (100km from unnao)…….. 37

6.1 Three bus test system 38

6.2 SMIB model 39

6.3 Speed variation of SMIB machine during stable and unstable power swings 41

6.4 Relative speed of SMIB machine obtained in accordance with proposed Algorithm 42

6.5 Relative speed of SMIB machine obtained in accordance with proposed Algorithm 43

Chapter 1

INTRODUCTION

Reliability is one of the prominent factors in operation of power systems that has notable economic impact and influence on society. Historically, power systems have been remarkably reliable. Although minor outages have been common, large-scale and wide-spread outages rarely happened and interruptions have occurred over relatively limited area. However, changes in the wholesale electricity market alongside the difficulties in upgrading the transmission systems have caused power systems to face more challenging network wide issues. In this condition, a minor disturbance can be intensified by a series of events leading to network wide effect. Subsequently, system may completely collapse, if timely actions are not adopted .

The current Supervisory Control and Data Acquisition (SCADA) systems observe grid conditions every few seconds. Thus they are incapable of providing information about the dynamic state of the power system. In addition, SCADA data are not consistently time-synchronized and shared widely across the network. Therefore, SCADA does not provide operators with real-time and wide-area visibility. The emergence of PMUs provides a significant improvement in reliability by offering unprecedented time-synchronized and high resolution information over a wide-area, in realtime known as wide area monitoring system (WAMS). Many advanced smart grid applications can take advantage of the measurement capabilities of PMUs.These applications enable utilities to react promptly to contingencies and prevent large-scale blackouts.

1.1 WIDE AREA MONITORING SYSTEM (WAMS)

Wide area monitoring systems (WAMS) are essentially based on the new data acquisition technology of phasor measurement and allow monitoring of power system conditions over large area.WAMS helps the power system operators to continuously analyse all the features of a power network in real time.

It is a concept that involves the use of system wide information and communication of selected local information to a remote location to counteract the propagation of large disturbances.WAMS requires accurate phasor and frequency information from multiple synchronised devices.

1.2 ARCHITECTURE OF WAMS

Synchronised measurement technology (SMT) is an important element and enabler of WAMS . It is supported by GPS . Its main building blocks are :

i. PMU (phasor measurement unit)
ii. Data concentrators (DC)
iii. Application softwares
iv. Supporting communication network

A PMU-based WAMS is a system in which PMUs measure power system parameters including frequency, voltage, and current phasorswith high accuracy. Meanwhile, each phasor is time-stamped using signals from Global Positioning System (GPS) so that the microsecond when the measurement taken is permanently attached to it. Afterwards, the timecritical phasor data are collected from various locations in the electrical grid and will be transmitted to a central location called Phasor Data Concentrator (PDC). A PDC receives and time-synchronizes phasor data from geographically distributed PMUs and produces a real-time, time-aligned output data stream. This information will be exploited by smart grid applications . These applications are generally categorized as on-line or off-line. On-line applications process real-time data as it arrives to the client system. In contrast, off-line applications process data that is archived .

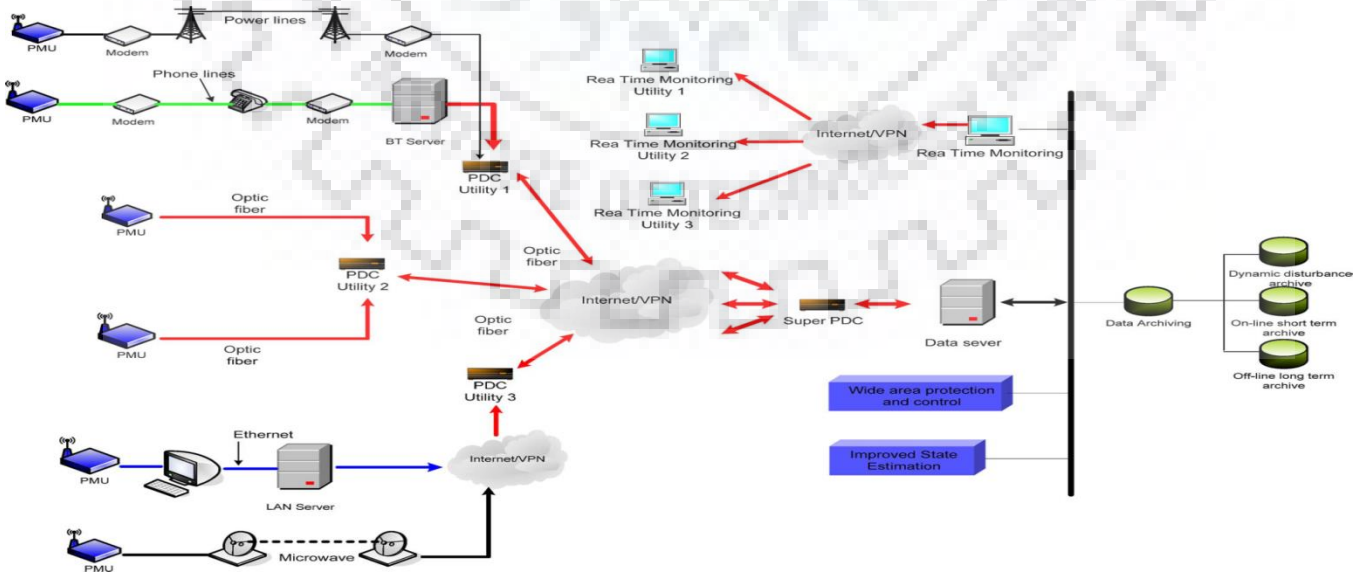

Fig 1.1 : WAMS basic architecture

1.3 Benefits of WAMS

- Reduced system instability
- Increased the capacity and profitability
- Increased interoperability
- High performance and improved adaptability
- Simplified system management

Chapter- 2

Phasor Measurement unit (PMU)

2.1 Phasor

A phasor is a mathematical representation of an electrical waveform based on the amplitude and phase angle. Use of the phasor notation considerably simplifies not only the mathematics but also the electronics and processing requirement [6]. The most common technique for determining phasor representation of AC waveforms is to take data samples from the waveform using an analog to digital converter and apply the Discrete Fourier Transform (DFT).

Time synchronization of phasors is necessary in order to obtain a complete view of the grid at specific time and to make the comparison of measurements from PMUs installed at different geographical locations more accurate. Synchronized phasors are known as synchrophasors.A phasor can be represented mathematically by the equqtion

$$x(t) = X_m \cos(\omega t + \phi) \qquad \text{Eqn 1}$$

where: X_m = magnitude of the sinusoidal waveform

$\omega = 2 * \pi * f$ where f is the instantaneous frequency

ϕ = angular starting point for the waveform

In a phasor notation, this waveform is typically represented as

$$X = X_m \angle \phi$$

Rotating vectors are used to describe ac circuits which are characterised by magnitude and phase.By definition they rotate counter-clockwise .

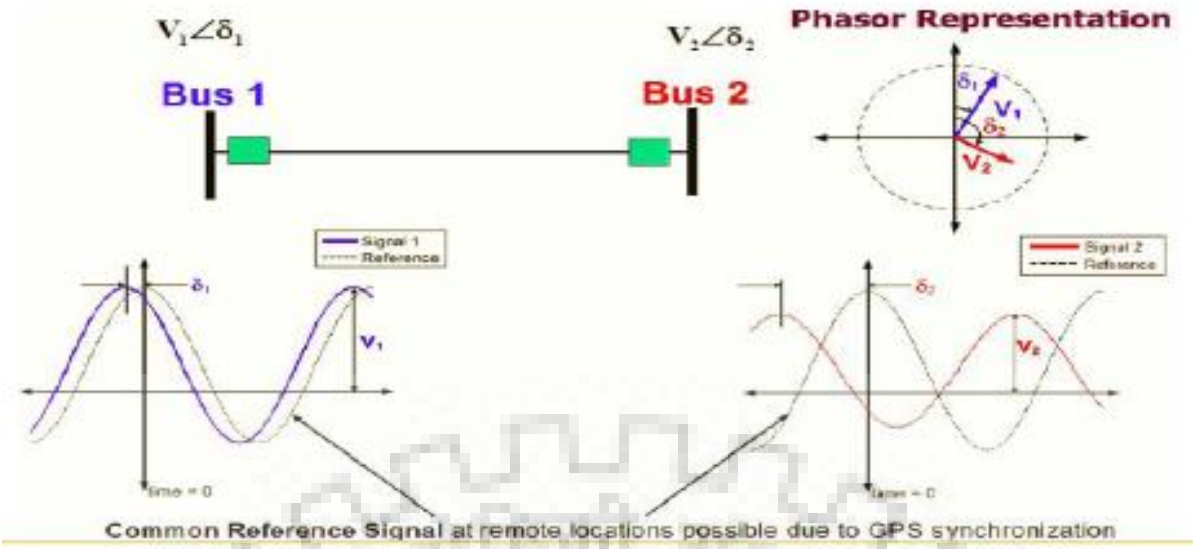

Fig 2.1: Phasor representation

PMUs require a precise time input. This synchronization is achieved by using a sampling clock which is phase-locked to the one-pulse-per-second signal provided by a GPS receiver . Most PMUs use a direct GPS input from an antenna or an IRIG-B time code. It is possible to use one GPS antenna for more than one PMU by using GPS antenna splitter.

2.2 IEEE Standard for SynchrophasorMeasurements

i. IEEE C37.118™-2005
ii. IEEE C37.118.1™-2011
iii. IEEE C37.118.1a™-2014

i. IEEE C37.118™-2005:This standard defines synchronized phasor measurements used in power system applications and provides a method to quantify the measurement. It also defines a data communication protocol, including message formats for communicating this data in a real-time system.

ii. IEEE C37.118.1™-2011: This standard defines synchrophasors, frequency, and rate of change of frequency (ROCOF) measurement under all operating conditions. It specifies methods for evaluating these measurements and requirements for compliance with the standard under both steady-state and dynamic conditions.

iii. IEEE C37.118.1a™-2014:Modifications in this amendment include some performance requirements with related text updates to correct inconsistencies and remove limitations introduced by IEEE Std C37.118.1(TM)-2011.

2.2 PMU Installation

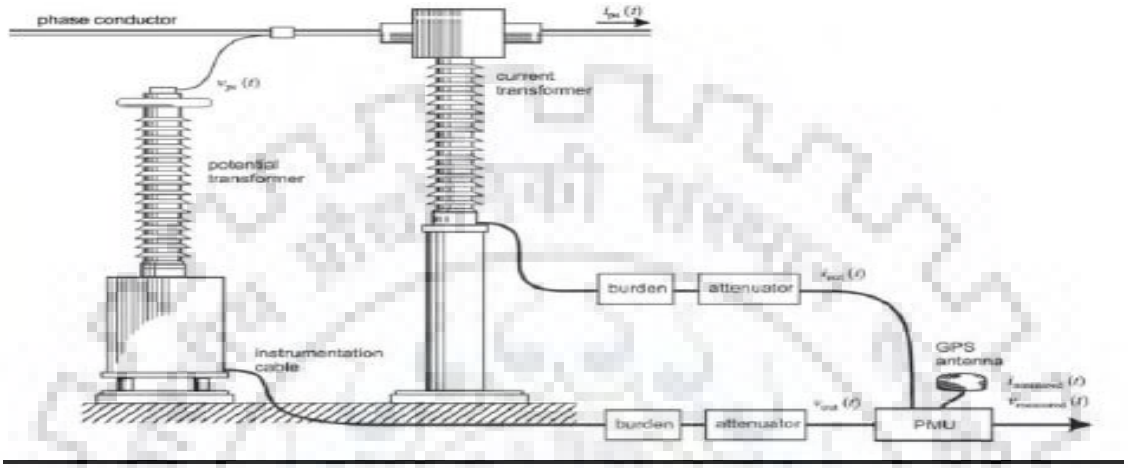

Fig 2.2 : PMU connection

In most cases, PMU installation is for a permanent operation so all aspects should be considered in order to have a well-established measurement system. PMUs can be different in the matter of algorithm selection, timing input, number of voltage and current inputs, communication interface, accuracy, etc.. However, they have number of common requirements, including: access to signals to be measured, a timing signal to synchronize the measurements, and a power supply .

PMUs need to have access to the voltage and current signals to be measured. In some substations these signals are available in a single location, while in many substations these signals are brought to the different buildings or cabinets. In this condition, it may be necessary to include several PMUs or use a PMU that has distributable input modules to cover the whole substation . The analog input signals corresponding to voltages and currents are obtained from the instrument transformers as shown in Figure 3. Several instrument transformer technologies are available that can be used to transform signals to an appropriate level for PMU applications. It should be noted that the measurement accuracy of PMU is directly affected by the instrument transformers .

2.4 PMU Hardware block diagram

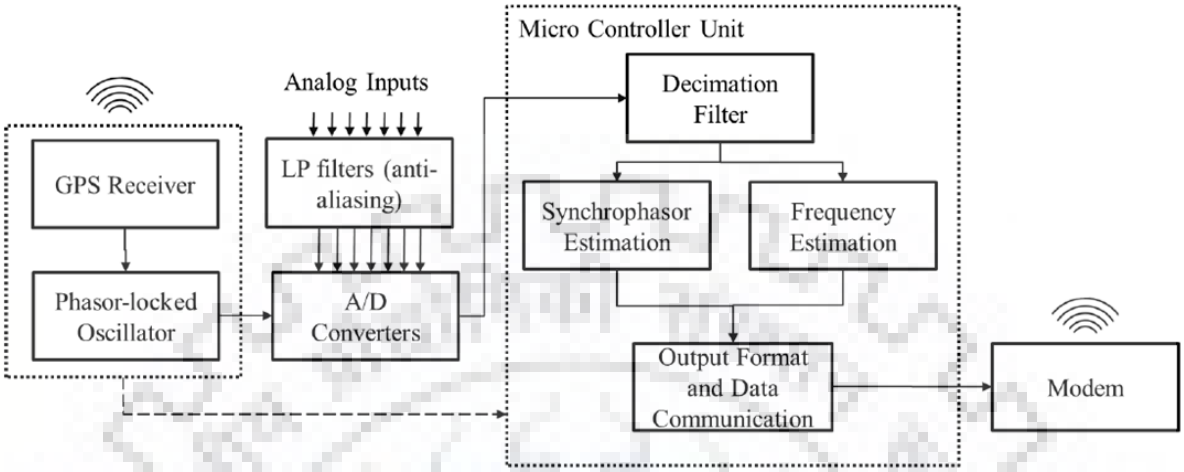

Fig 2.3 : PMU hardware block diagram

2.5 Performance criteria of PMU

- Accuracy for the Synchrophasor is measured by a value termed the "Total Vector Error" or TVE.
- TVE is defined as the square root of the difference squared between the real and imaginary parts of the theoretical actual phasor and the estimated phasor to the ratio of magnitude of the theoretical phasor and presented as a percentage.

$$\varepsilon = (\sqrt{[(X_r(n) - X_r)^2 + (X_i(n) - X_i)^2) / (X_r^2 + X_i^2)]}) * 100 \quad \text{Eqn. 2}$$

where: X_r and X_i represent the theoretical exact synchrophasor

and: $X_r(n)$ and $X_i(n)$ represent the estimated synchrophasor

- Phasor Measurement Unit (PMU) must maintain less than a 1% TVE under conditions of ±5 Hz of off-nominal frequency, 10% Total Harmonic Distortion.

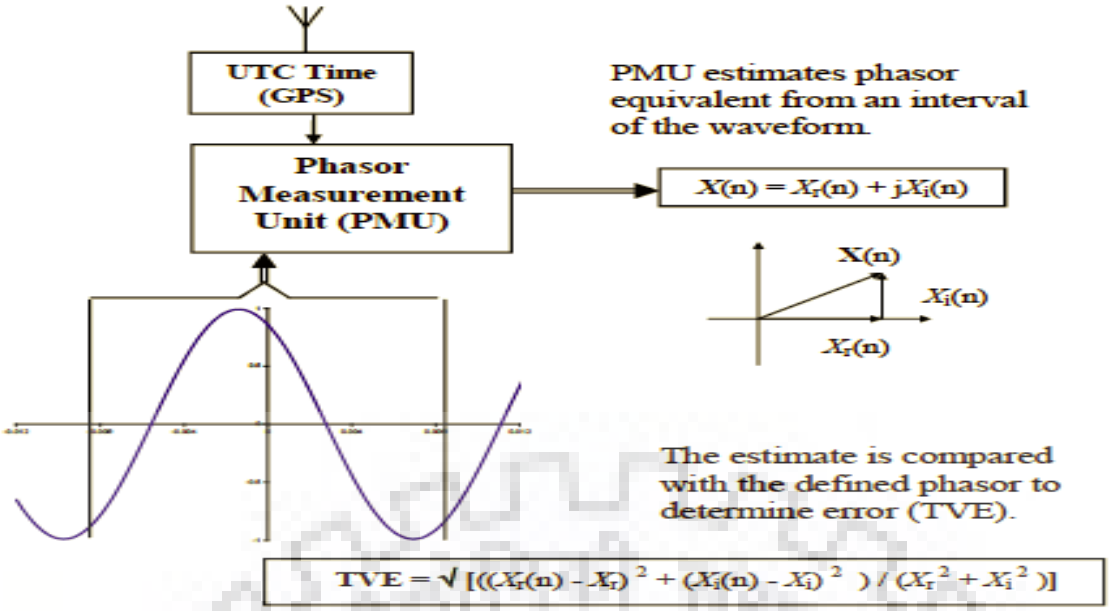

Fig 2.4 : Measurement of TVE

2.6 PMU Challenges

- Visualization of PMU data – Difficult to visualize and manage large amounts of data.
- Communication of PMU data – Expensive communication network required.
- Optimal Placing of PMU's.
- High investment.
- Diverse requirements from the utilities.

Chapter-3

OTHER COMPONENTS OF WAMS

3.1 Phasor Data Concentrators

IEEE C37.118 standard defines four message types: data, configuration, header and command. The first three message types are transmitted from the data source, PMU or PDC, and the last one is received by the data source. It should be noted that PDC itself can be considered as a data source when it sends data to another PDC . Data messages cannot stand alone, as they do not describe the data they contain. Configuration messages contain information required to determine the meaning of each individual field with the data message .

A typical exchange between a PMU and a PDC is as following :

- The PDC sends a command message to the PMU to request human-readable description information
- The PMU replies with a header message
- The PDC sends a command message to the PMU to request configuration information
- The PMU replies with a configuration message
- The PDC sends a command message to the PMU to request data
- The PMU replies with data messages until the PDC sends a command message to terminate its request

A PDC collects data from multiple PMUs or other PDCs and time-aligns phasor data according to their time-stamps. In fact, it forms a data packet with a given time-stamp, and then assembles all data received with that time-stamp into the single packet. The produced real-time and synchronized output data stream can be exploited by smart grid applications and is also stored for future analysis. A high number of PMUs are installed in the whole power systems and they depend on the limited number of PDCs to process and store their data. Therefore, each PDC needs to deal with huge amount of data and the required data storage capacity should be considered. As more PMUs are deployed in the system, the number of measurement samples increases and the storage requirement accelerates . Storing and processing a huge volume of PMUs measurements and scanning through terabytes of information to find the particular event will be a big challenge for WAMS.

3.2 Communication Network

In developing a WAMS, reliable and high speed communication infrastructure that enables secure sharing of data among PMUs, PDCs and smart grid applications play an important role. IEEE C37.118 frames are typically not sent directly over network, but rather based on the concept of layered protocols they are encapsulated within frames of other communication protocols . The speed of data transfer is less critical for the off-line applications, while for the on-line applications a faster data transfer is required and depends on the type of application. The communication infrastructure should therefore be able to support different Quality-of-Services (QoS) classes for traffic and should be able to prioritize one class over another . Most PMUs have an Ethernet interface, although there are some models that only use asynchronous serial (RS 232). An interface device (modem, Router, etc.) is required between the PMU communication link and the communication system. Communication over network using Internet Protocol (IP) can be connection-oriented (TCP) or connectionless (UDP). TCP rearranges data packets in the order specified and retransmitslost or corrupted data. In the case of UDP there is no built-inordering and recovery of data, but the transmission speed is higher than TCP. Therefore, UDP is used commonly with PMUs since a small amount of lost data is preferable over delayed data in many real time smart grid applications.

Many utilities today use Multi-Protocol Label Switching (MPLS) Virtual Private Networks (VPNs), or Frame Relay technology for WANs. These communication media provide a guaranteed bit rate but are not guaranteed to be error free . Since data may be shared with multiple entities at the same time and for communication redundancy, a WAMS should also support multicast data sharing.

3.3 WAMS APPLICATIONS FOR POWER SYSTEMS

WAMS brings great potential for improving reliability and stability based on the operational feature of the PMUs. In the literatures, there are a large number of WAMS applications; however they can be categorized into three main groups of monitoring, protection, and control applications .

A. **Power System Monitoring:** A PMU-based monitoring systems offer various kinds of functions, such as wide area visualisation, model validation, state estimation, near real-time event replay, post event analysis, early warning of potential problems etc. These functionalities will significantly improve situational awareness. When power system operates in a normal condition, providing applications with reduced resolution synchro phasor measurements is sufficient. However, for the near real-time event replay mode and post event analysis, measurements with full resolution are required .

B. Power System Protection: Synchronized phasor measurements offer solution to a number of complex protection problems and improve the performance of the protection applications. Phasor measurements are particularly effective in enhancing power system protection functions that have a slow response time requirement. Some protection systems that could benefit from PMUs include: adaptive dependability and security, back up protection of distance relays, adaptive out-of-step, angular voltage stability of network, etc .

C. Power system control: Prior to the emergence of real-time phasor measurements most of the control systems were processed locally due to low time delay. Controllers like variable series capacitor (VSC), universal power flow controllers (UPFCs) and power system stabilizers regulate the grid based on a local feedback. While phasor measurements in addition to remote control of the power systems, could provide direct feedback to these controllers and enable dynamic control of the power systems. Using PMUs to damp the low frequency inter-area oscillations is one of the effective applications of WAMS

3.4 Real Time Dynamics Monitoring System (RTDMS)

RTDMS is a Synchrophasor software application for providing real time, wide area situational awareness to Operators, Reliability Coordinators, Planners and Operating Engineers, as well as the capability to monitor and analyse the dynamics of the power system.

RTDMS provides critical metrics of grid dynamics, like

1. Phase Angle Differences
2. Small Signal Stability (Oscillations & Damping)
3. Frequency Instability
4. Generation-load imbalance
5. Power-Angle Sensitivity

Chapter- 4

PMU MODEL IN MATLAB/SIMULINK

In this chapter we discuss this advanced technology (PMUs) with the help of MATLAB simulation. We design this PMU model in MATLAB SIMULINK and then we installed this model in the start and end of transmission line in our sample simulation of a small power system in SIMULINK. This all is for testing of its testing valuation. Such application is made for the protection, monitoring and control of wide power system.

PMU Mathematical Model

Following mathematical model is used to calculate the magnitude and phase angles of voltages and currents.

$$v(t)= \cos(\omega t + \phi)$$

$$\omega = 2 \Pi f$$

$$g(t) = y(t) - y\left(t - \frac{1}{f}\right)$$

$$y(t) = \int u(t)\, dt$$

$$u(t) = \sin(t) * v * 2 * 50$$

Now for real part

$$y(t) = 100 \int v(t) * \sin(t)\, dt$$

$$y(t) = 100\left(v(t)*(-\cos(t))\right) - \int \left(\frac{d}{dt} v(t) * \int \sin(t)\, dt\right) dt$$

$$y(t) = 100\left(v(t)*\left(-\cos(t)\right)\right) - \int\left(\frac{d}{dt}v(t)*\int \sin(t)dt\right)dt$$

Now

$$y(t) = 100\int v(t)*\sin(t)dt$$

$$= \left(\frac{1}{1-\omega^2}\right)\left(-100*v(t)*\cos(t)\right.$$

$$\left.-100(\omega)\sin(\omega t+\phi)*\sin(t)\right)$$

$$y\left(t-\frac{1}{f}\right)=100\int v\left(t-\frac{1}{f}\right)*\sin\left(t-\frac{1}{f}\right)dt$$
$$=\left(\frac{1}{1-\omega^2}\right)\left(-100*\cos\left(\omega\left(t-\frac{1}{f}\right)\right)\right.$$
$$*\cos\left(t-\frac{1}{f}\right)-100(\omega)\sin\left(\omega\left(t-\frac{1}{f}\right)+\phi\right) \quad (3)$$
$$\left.*\sin\left(t-\frac{1}{f}\right)\right)$$

$$g(t)=y(t)-y\left(t-\frac{1}{f}\right)=\left(\frac{1}{1-\omega^2}\right)$$
$$\left(-100*v(t)*\cos(t)-100(\omega)\sin(\omega t+\phi)\right)$$
$$*\sin(t)-\left(\frac{1}{1-\omega^2}\right)\left(-100*\cos\left(\omega\left(t-\frac{1}{f}\right)\right)\right)$$
$$*\cos\left(t-\frac{1}{f}\right)-100(\omega)\sin\left(\omega\left(t-\frac{1}{f}\right)+\phi\right)$$
$$\left.*\sin\left(t-\frac{1}{f}\right)\right)$$

For imaginary part :

$$y(t)=\int u(t)\,dt$$
$$u(t)=\cos(t)*v(t)*2*50$$
$$y(t)=100y(t)=100\int v(t)*\cos(t)\,dt$$
$$k(t)=y(t)-y\left(t-\frac{1}{f}\right) \quad (4)$$
$$y(t)=100\int v(t)*\cos(t)\,dt$$
$$=100\cos(\omega t+\phi)*\sin(t)$$
$$-\int-\sin(\omega t+\phi)*\omega\left(\sin(t)\,dt\right)$$

$$y(t)=\left(\frac{1}{1-\omega^2}\right)(100*v(t)*\sin(t) \quad (5)$$
$$-100(\omega)\sin(\omega t+\phi)*\cos(t))$$

$$y\left(t-\frac{1}{f}\right)=\left(\frac{1}{1-\omega^2}\right)\left(100*v\left(t-\frac{1}{f}\right)\right. \quad (6)$$
$$\left.-100(\omega)*\sin\left(\omega\left(t-\frac{1}{f}\right)+\phi\right)*\cos\left(t-\frac{1}{f}\right)\right)$$

Put Equations (5) and (6) in Equation (4) so

$$k(t)=y(t)-y\left(t-\frac{1}{f}\right)$$

Put Equations (5) and (6) in equation (4) so

$$k(t) = y(t) - y\left(t - \frac{1}{f}\right)$$

$$y(t) = \left(\frac{1}{1-\omega^2}\right)(100 * v(t) * \sin(t)$$
$$-100(\omega)\sin(\omega t + \phi) * \cos(t))$$
$$-\left(\frac{1}{1-\omega^2}\right)\left(100 * v\left(t - \frac{1}{f}\right)\right.$$
$$\left.-100(\omega)\sin\left(\omega\left(t - \frac{1}{f}\right) + \phi\right) * \cos\left(t - \frac{1}{f}\right)\right)$$

Now for magnitude and phase angle :

$$\text{Magnitude} = \sqrt{(g(t))^2 + (y(t))^2}$$

$$\text{Phase} = \tan^{-1}\left(\frac{\text{Equation 4}}{\text{Equation 1}}\right)$$

In this matematical model we calculated real and imaginary part separately and then from it we calculated magnitude and phase.

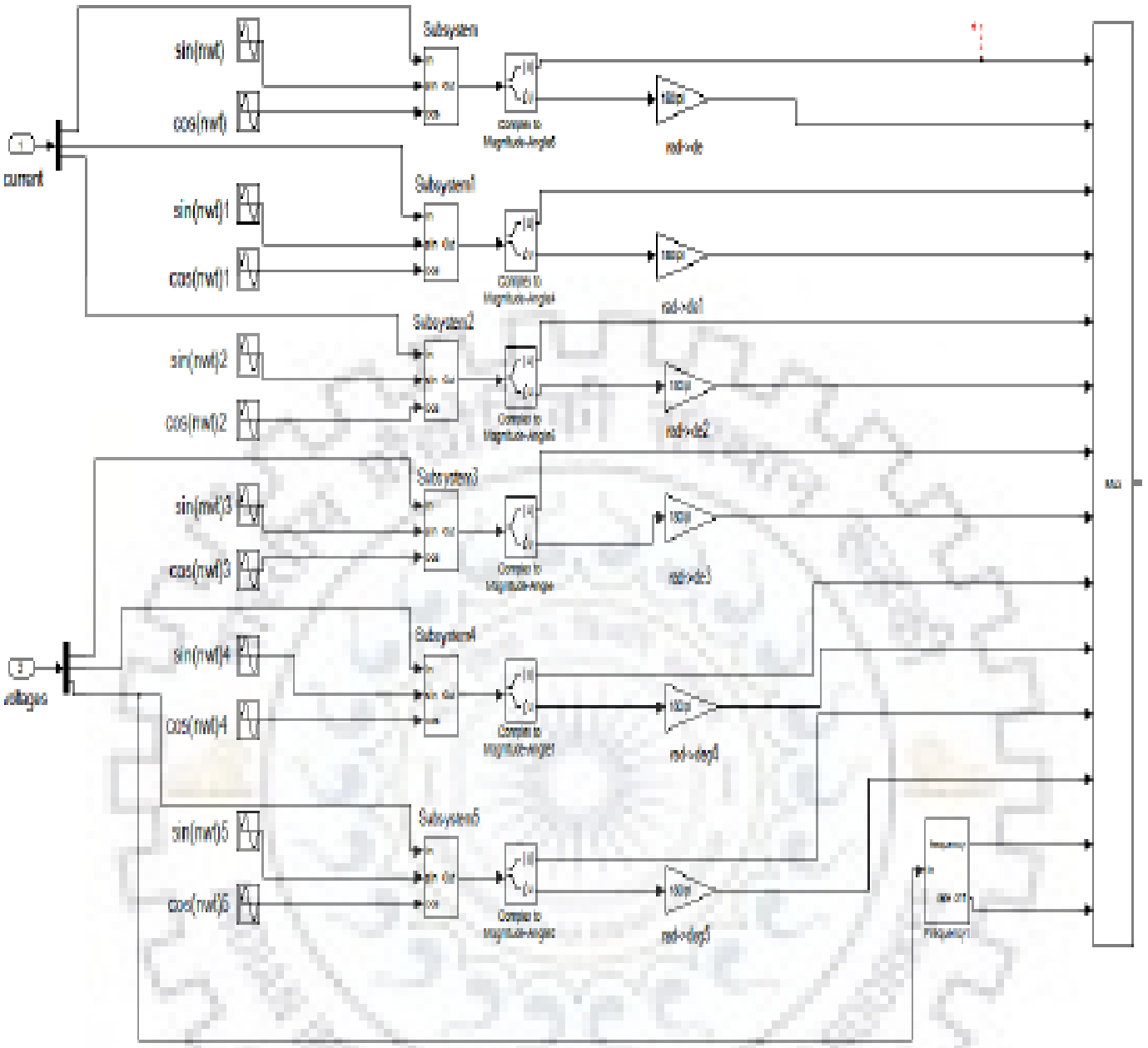

Fig 4.1 : PMU simulink Block diagram

WAMS MAIN SIMULINK BLOCK DIAGRAM

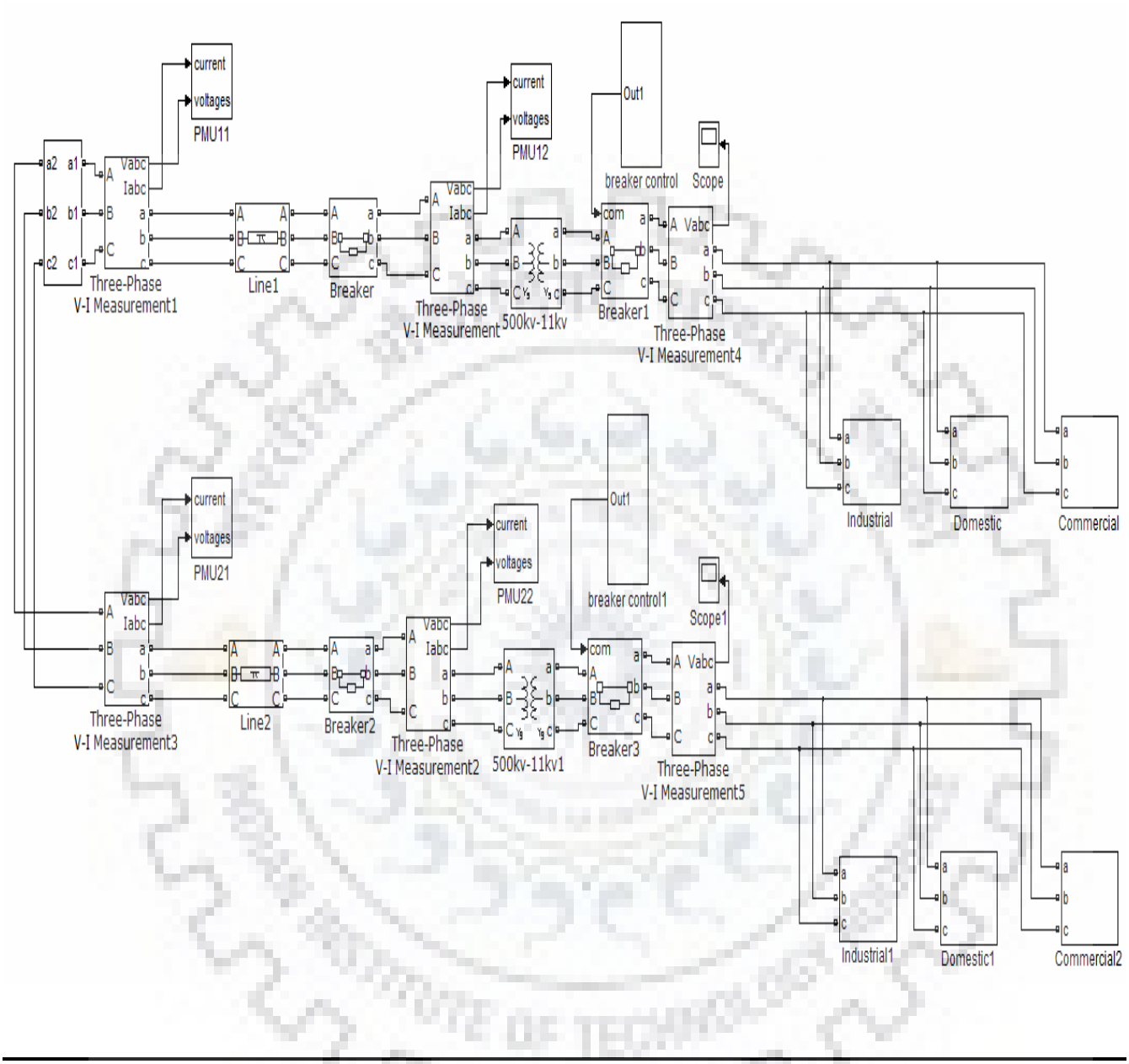

Fig 4.2 Wams Main Simulink Block Diagram

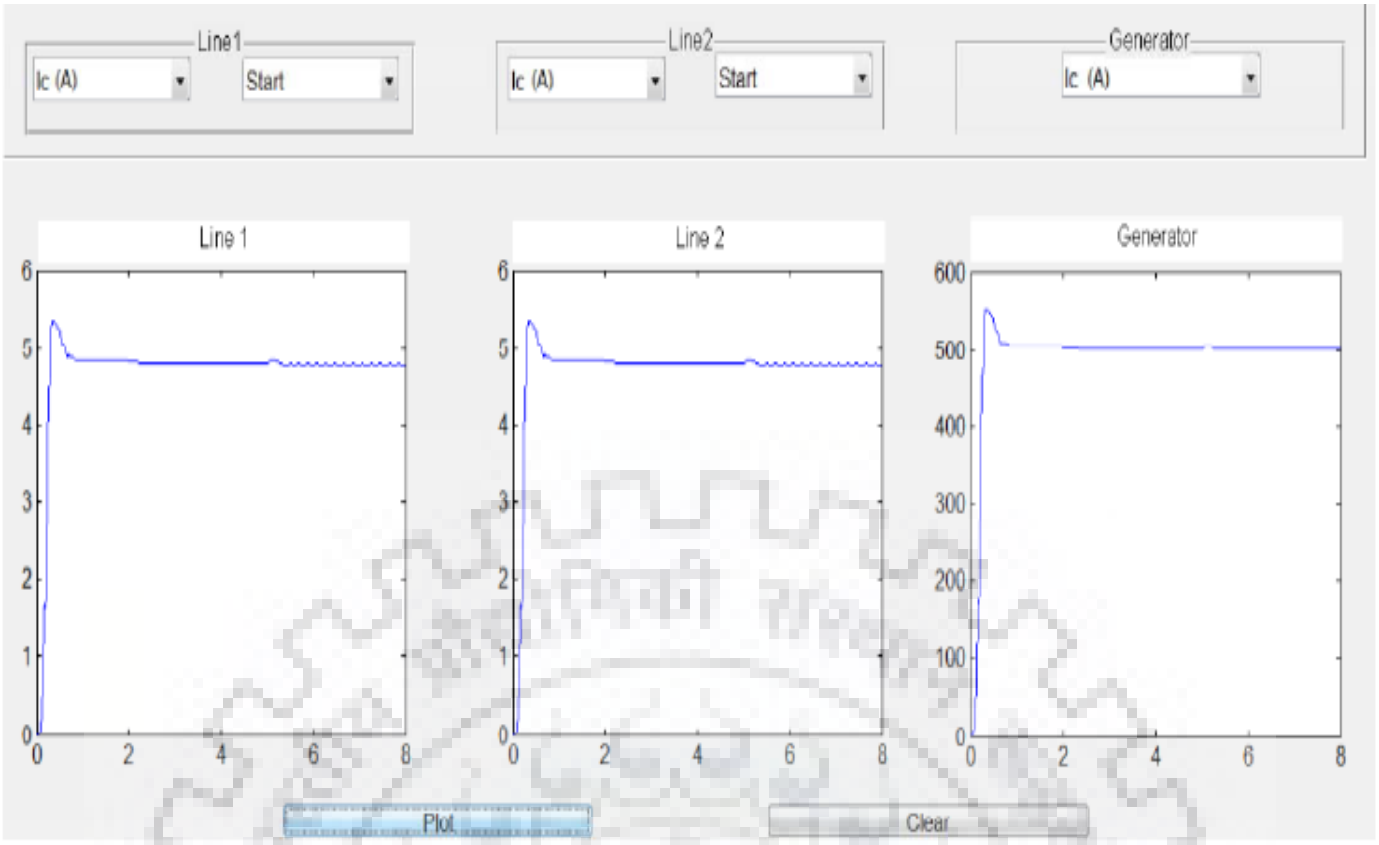

Fig 4.3 : CURRENT MAGNITUDE MEASUREMENT

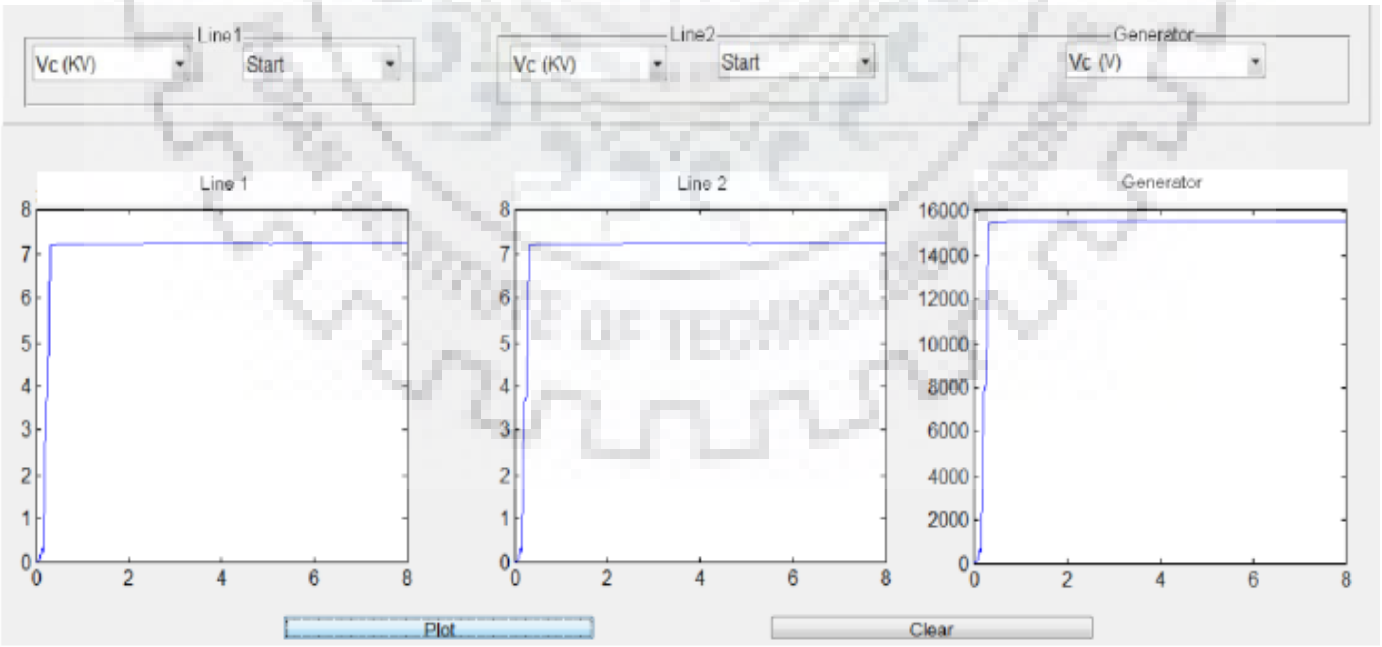

Fig 4.4 : Voltage Magnitude Measurement

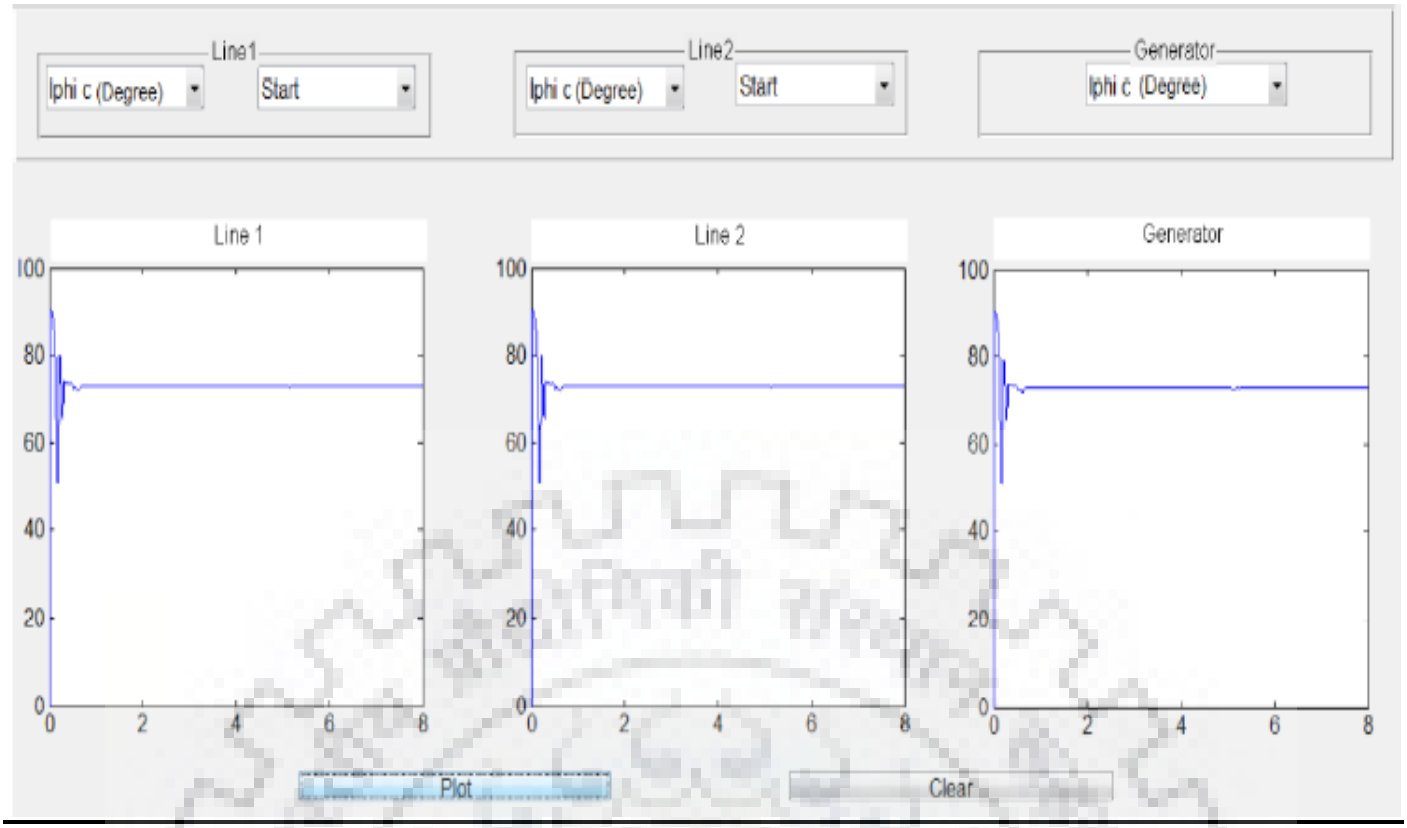

Fig 4.5 : Current Phase Angle Measurement

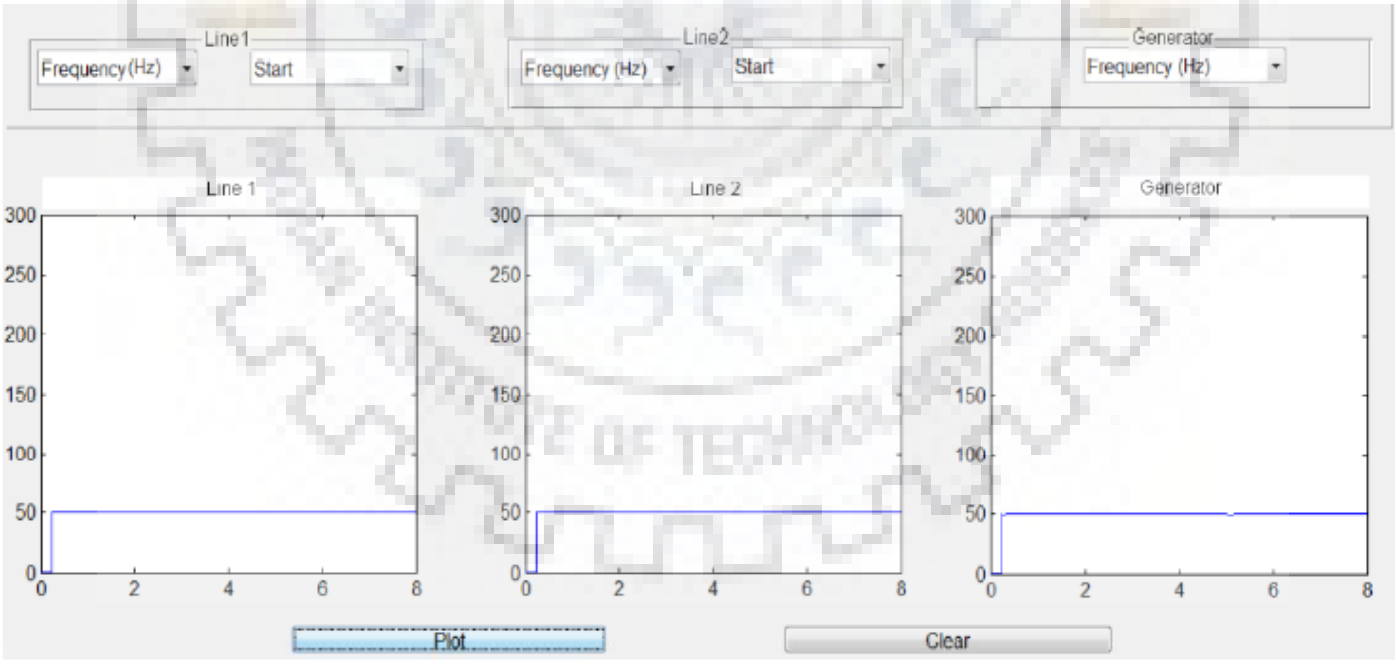

Fig 4.6 : Frequency Measurement

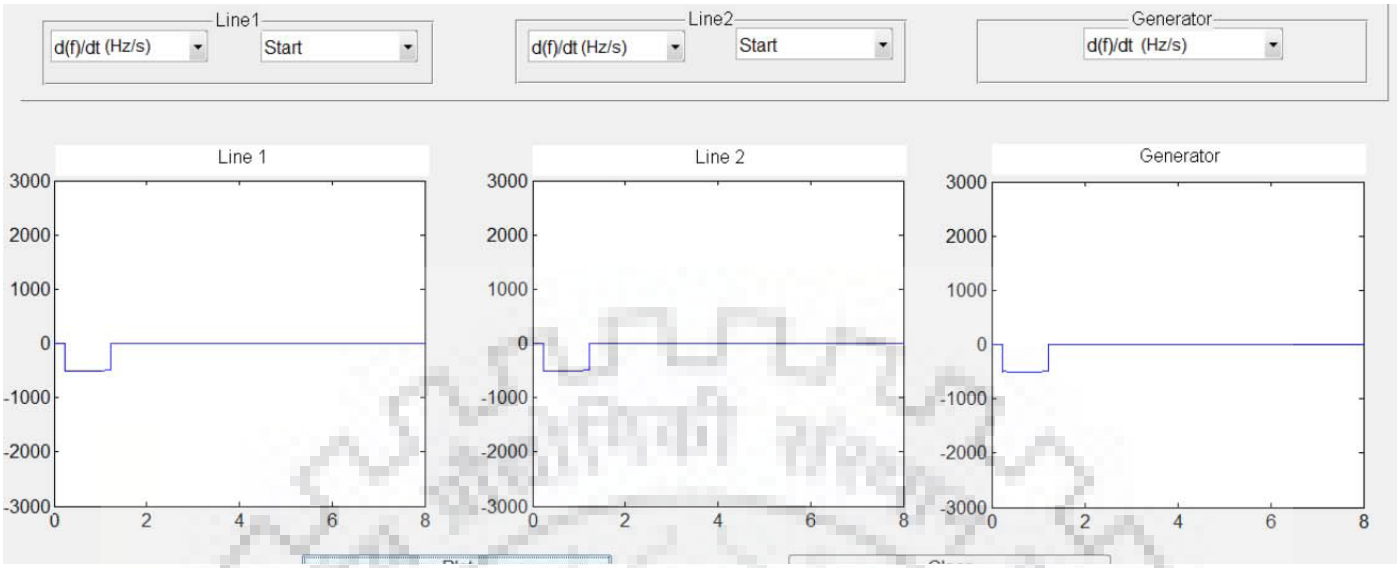

Fig 4.7: Rate of change of frequency

CHAPTER – 5

PMU DATA BASED FAULT LOCATION

In this chapter we will discuss the PMU based fault location techniqes.Fault location techniques based on the tavelling wave methods were developed in 1950s but these methods required very high sampling rate since travelling waves travels at a speed slightly less than the speed of light.With the development in PMU and impedence based fault location method the sampling rate required got reduced. Here we have used two techniques for calculating the fault location:

1) Two ended negative sequence impedence method

2)Two ended method based on ditributed parameter transmission line model

Two ended data of transmission line is assumed to be measured by PMU located at both the ends.One three phase and one single phase transmission line is tesdted in PSCAD.

5.1 Two ended negative sequence impedence method

A negative sequence impedence method for fault location is particularly used for unbalanced faults to avoid the effects zero sequence mutual impedence , fault resistance etc. A one line two source circuit of a three phase transmission line is given below.

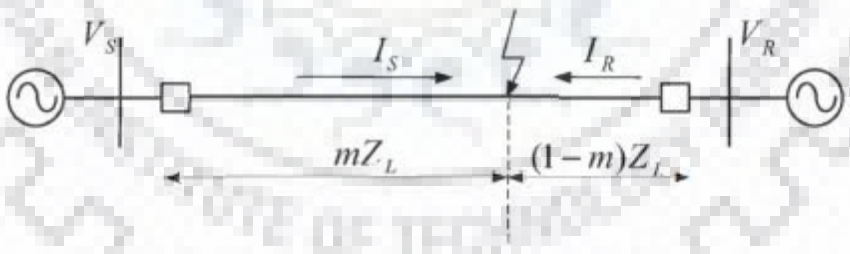

Fig. 5.1 : A one line two source circuit

In the above circuit m is the per unit fault distance. By using the sequence network of the one line two source network given in fig 5.2 we can calculate the fault voltage V_{2f}.

At relay S, we can write

$$V_{2f} = -I_{2S}(Z_{2S} + mZ_{2L})$$

At realy R wecan write

$$V_{2f} = -I_{2R}(Z_{2R} + (1-m)Z_{2L})$$

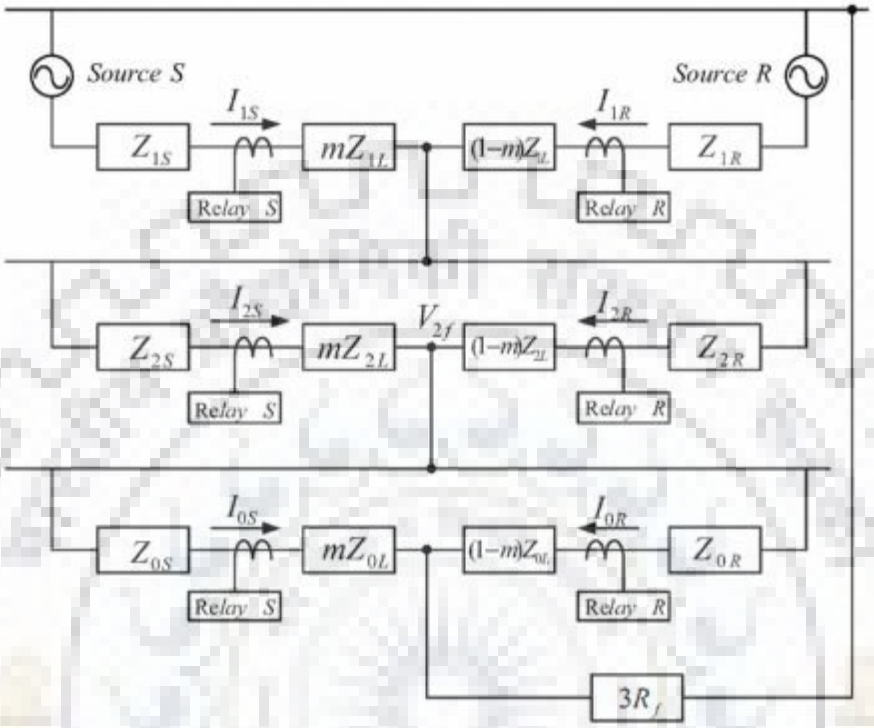

Fig 5.2 : Sequence network for single line two source circuit

From two values of fault voltage V_{2f}, we can write

$$I_{2R} = -I_{2S}\frac{Z_{2S} + mZ_{2L}}{Z_{2R} + (1-m)Z_{2L}}$$

By rearranging the above equation we can get,

$$\frac{|I_{2R}|}{|I_{2S}|} = \frac{|Z_{2S} + mZ_{2L}|}{|Z_{2R} + (1-m)Z_{2L}|}$$

If defines the impedence as follows :

$$Z_{2S} = a + j * b$$
$$Z_{2L} = c + j * d$$
$$Z_{2R} = e + j * f$$

Thus,

$$Am^2 + Bm + C = 0$$

Where,

$$A = (\frac{|I_{2R}|}{|I_{2S}|})^2(c^2 + d^2) - (c^2 + d^2)$$
$$B = -2(\frac{|I_{2R}|}{|I_{2S}|})^2(ce + df) - 2(ac + bd)$$
$$C = (\frac{|I_{2R}|}{|I_{2S}|})^2(e^2 + f^2) - (a^2 + b^2)$$

5.2 Simulation results for different fault locations for two ended negative sequence Impedence method :

A single line to ground fault (SLG) occured between phase A and ground (A-G fault) :

A SLG fault occurred for 0.2 seconds and time duration for fault is 0.05 seconds. The profiles of negative sequence current I_{2s} (sending end current) and I_{2r} (receiving end current) are also given. The system is tested for m=0, m=1, m=1/2, m=1/3, m=1/4 .

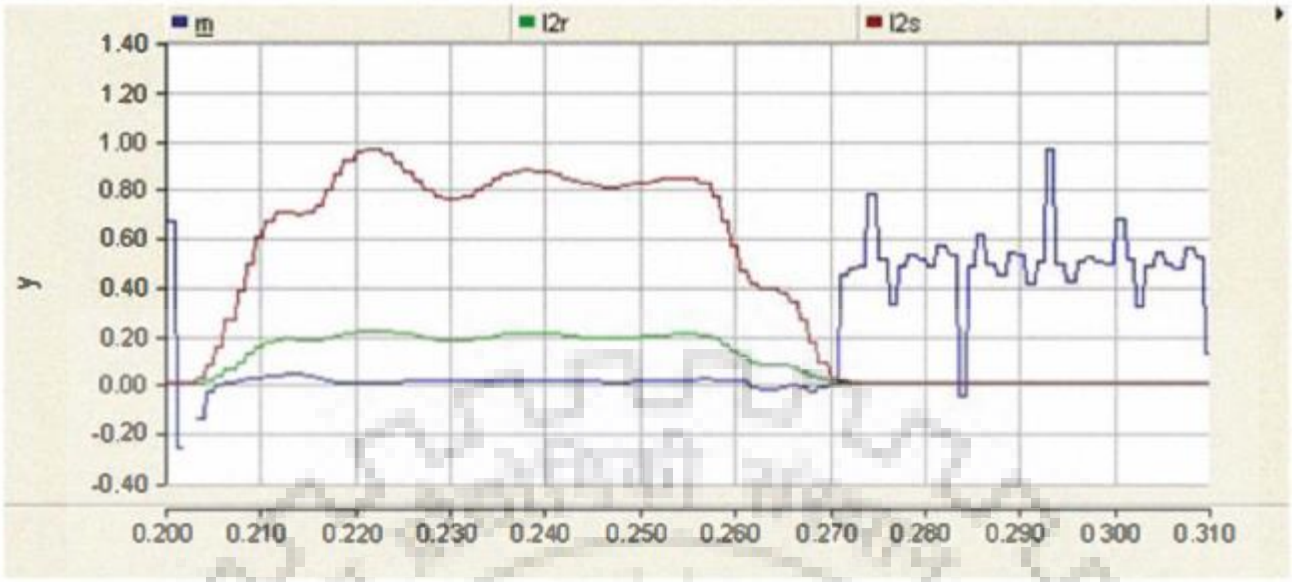

Fig 5.3 : SLG fault occurred at sending end (m=0)

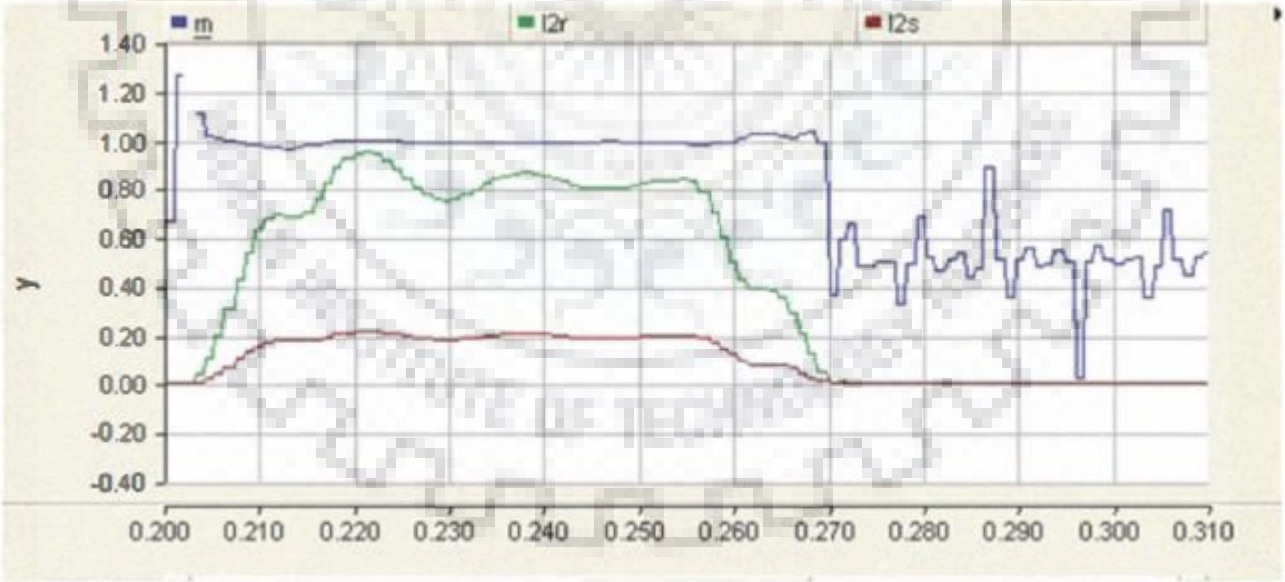

Fig 5.4 : SLG fault occurred at receiving end (m=1)

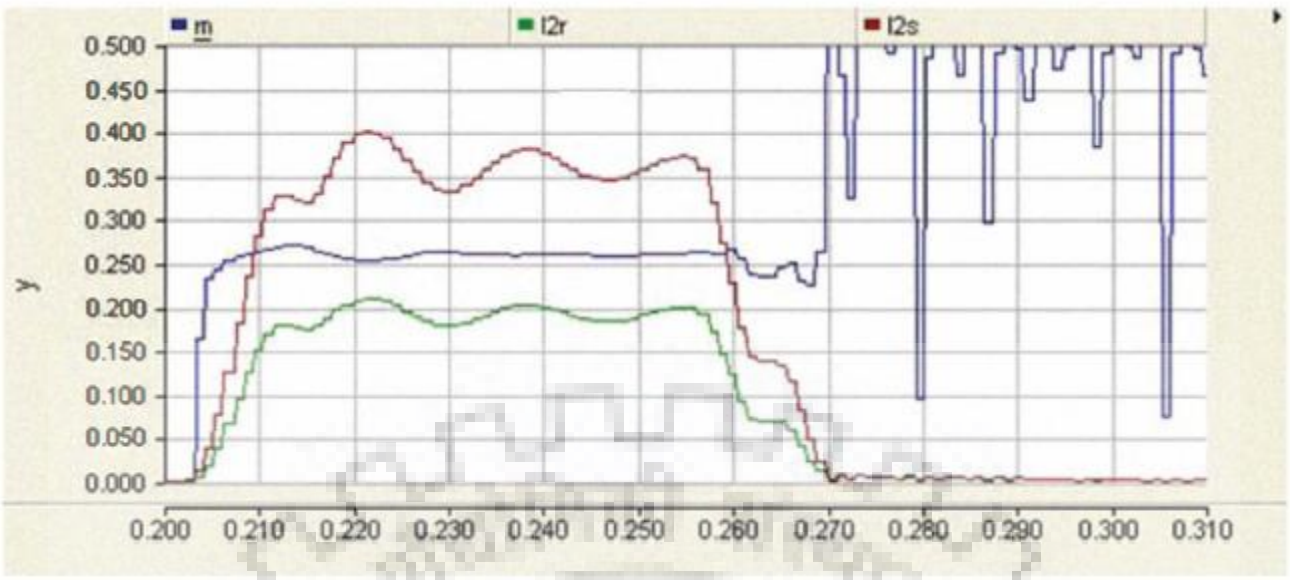

Fig 5.5 : SLG fault occurred at m=1/4

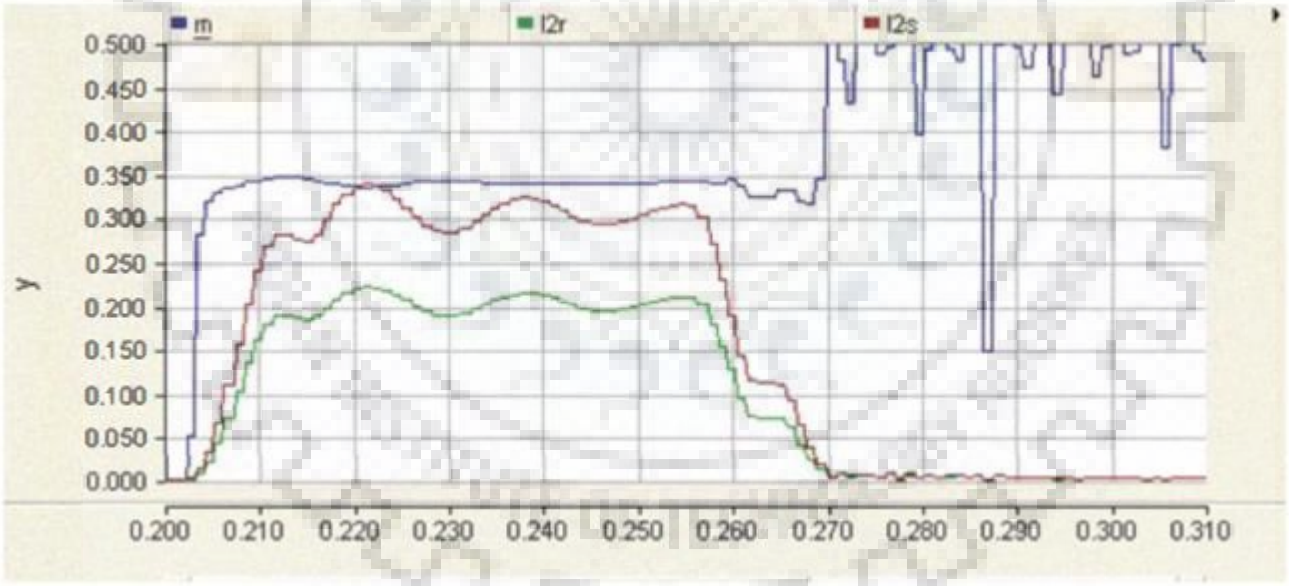

Fig 5.6 : Fault occurred at m=1/3

Fig 5.7 : Fault occurred at middle of line (m=1/2)

5.3 Two ended method based on distributed parameter transmission line model :

A two ended method based on distributed parameters transmission line model is proposed and discussed in this section. The voltages and currents of the transmission line are measured by the PMUs which are located at the ends of transmission line. A robust fault location index is derived for transmission line. Take a single-phase case for example, the fault location index is given as follow.

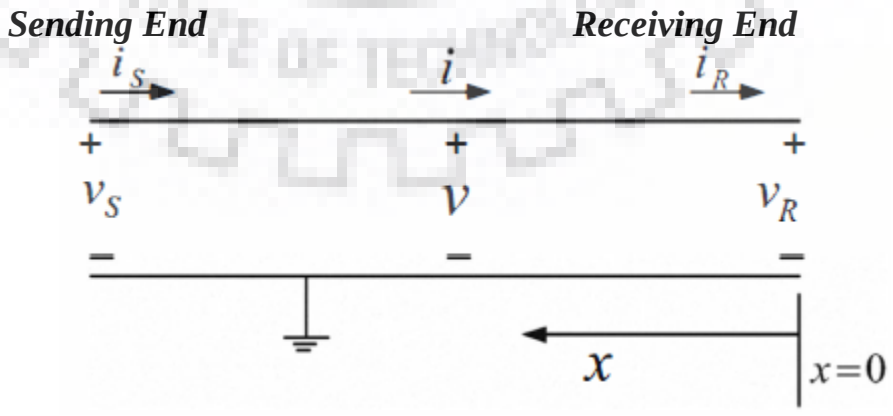

Fig 5.8 : One line two source circuit

The telegraph equation for circuit in fig 5.8 are as follows :

$$\frac{\partial v}{\partial x} = Ri + L\frac{\partial i}{\partial t}$$
$$\frac{\partial i}{\partial x} = Gv + C\frac{\partial v}{\partial t}$$

Where R,L,C,G are resistance,inductance,capacitance and conductance per unit length of transmission line.

The solutions of above telegraph equation are:

$$V = Ae^{\Gamma x} + Be^{-\Gamma x}$$
$$I = (Ae^{\Gamma x} - Be^{-\Gamma x})/Z_0$$

$$Z_0 = \sqrt{(R + j\omega L)/(G + j\omega C)}$$
$$\Gamma = \sqrt{(R + j\omega L) * (G + j\omega C)}$$

Zo is called the characteristic impedance, whose unit is Ω , Γ is the propagation cosntant, whose unit is m^{-1}.

A, B are the integration constants, which are determined by the boundary conditions of the transmission line.

At the receiving end (x=0),

$$V_R = A + B$$
$$I_R = (A - B)/Z_0$$

So,

$$A = (V_R + Z_0 I_R)/2$$
$$B = (V_R - Z_0 I_R)/2$$

At the sending end (x=L),

$$V_S = Ae^{\Gamma L} + Be^{-\Gamma L}$$
$$I_S = (Ae^{\Gamma L} - Be^{-\Gamma L})/Z_0$$

So,

$$A = \frac{V_S + Z_0 I_S}{2} e^{-\Gamma L}$$

$$B = \frac{V_S - Z_0 I_S}{2} e^{\Gamma L}$$

Thus, the voltage at x=DL could be expressed with (Vs, Is) or (V_R,I_R) ,

$$V_F = \frac{V_S + Z_0 I_S}{2} e^{-\Gamma L} e^{\Gamma DL} + \frac{V_S - Z_0 I_S}{2} e^{\Gamma L} e^{-\Gamma DL}$$

$$V_F = \frac{V_R + Z_0 I_R}{2} e^{\Gamma DL} + \frac{V_R - Z_0 I_R}{2} e^{-\Gamma DL}$$

Through above two eqations, fault location index can be calculated :

$$D = ln(N/M)/(2\Gamma L)$$

Where,

$$N = \frac{V_R - Z_0 I_R}{2} - \frac{V_S - Z_0 I_S}{2} e^{\Gamma L}$$

$$M = \frac{V_S + Z_0 I_S}{2} e^{-\Gamma L} - \frac{V_R + Z_0 I_R}{2}$$

5.4 Simulation result for different fault location based on Distributed parameter Transmission line method :

A simple one-phase transmission line with two sources is tested as shown in Fig. 5.9. A line-to-ground fault occurs at 0.2s and the duration time is 0.I5s. The detailed derivation process of the fault index D could be found in the part of fault Icoation based on distributed parameter transmission line method.

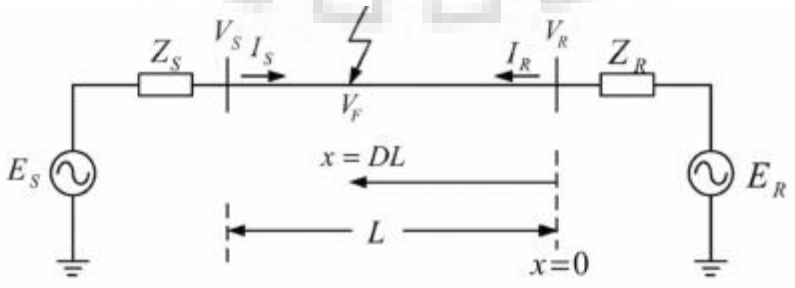

Fig 5.9 :Single phase faulted transmission line with two sources

Plots of the simulated D under three different fault locations (D = 1, D = 0.5, and D = 0.2) are shown in Fig 5.10 – Fig. 5.12 .Figures of the coefficients M and N are also given. The prefault absoulte values of M and N are zero. When the fault occurs, the absoulte values of M and N drivate from zero abruptly. And the fault index D converges to a value in the range of 0 and 1.

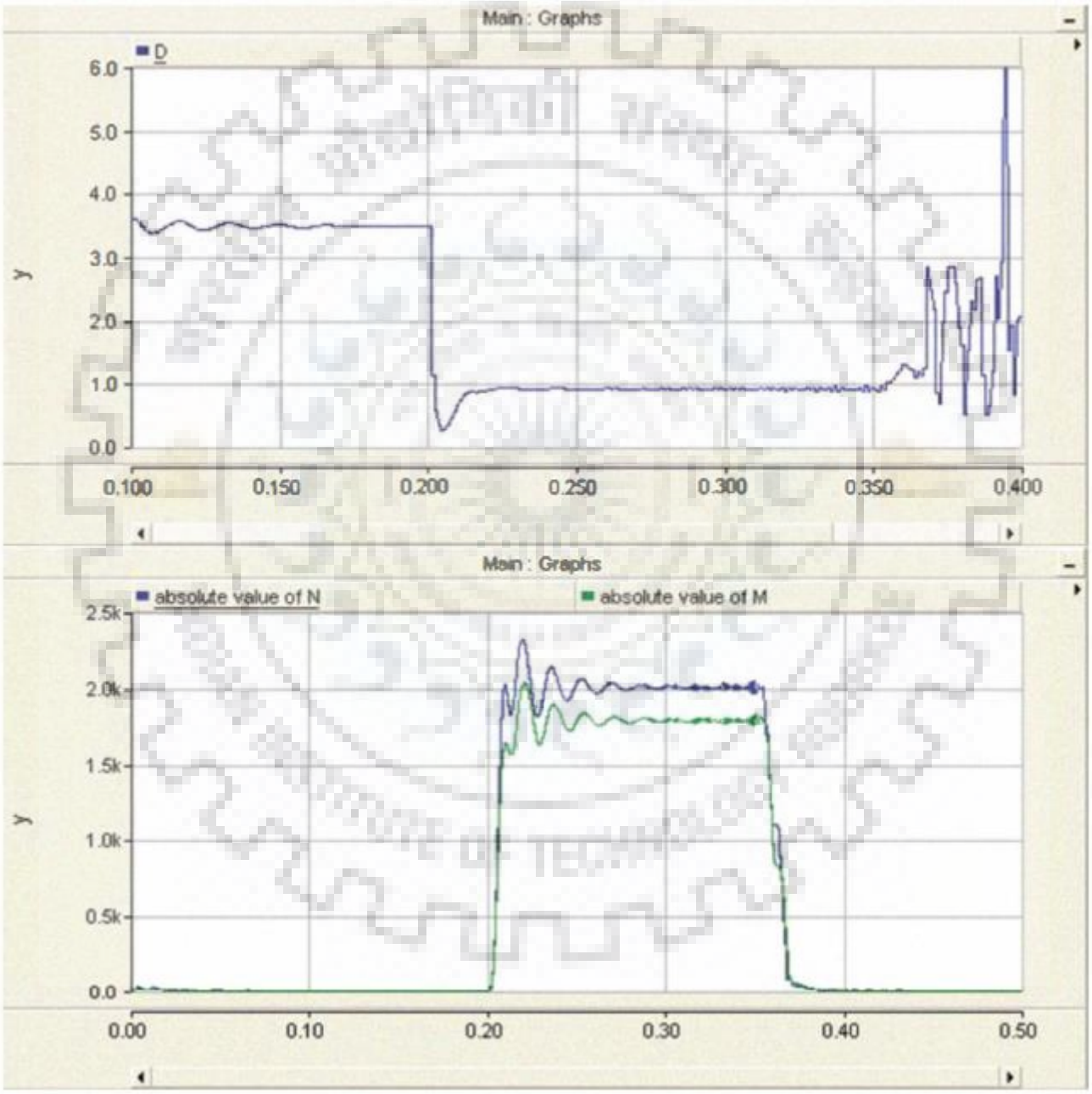

Fig. 5.10 : Single phase fault location with D=1

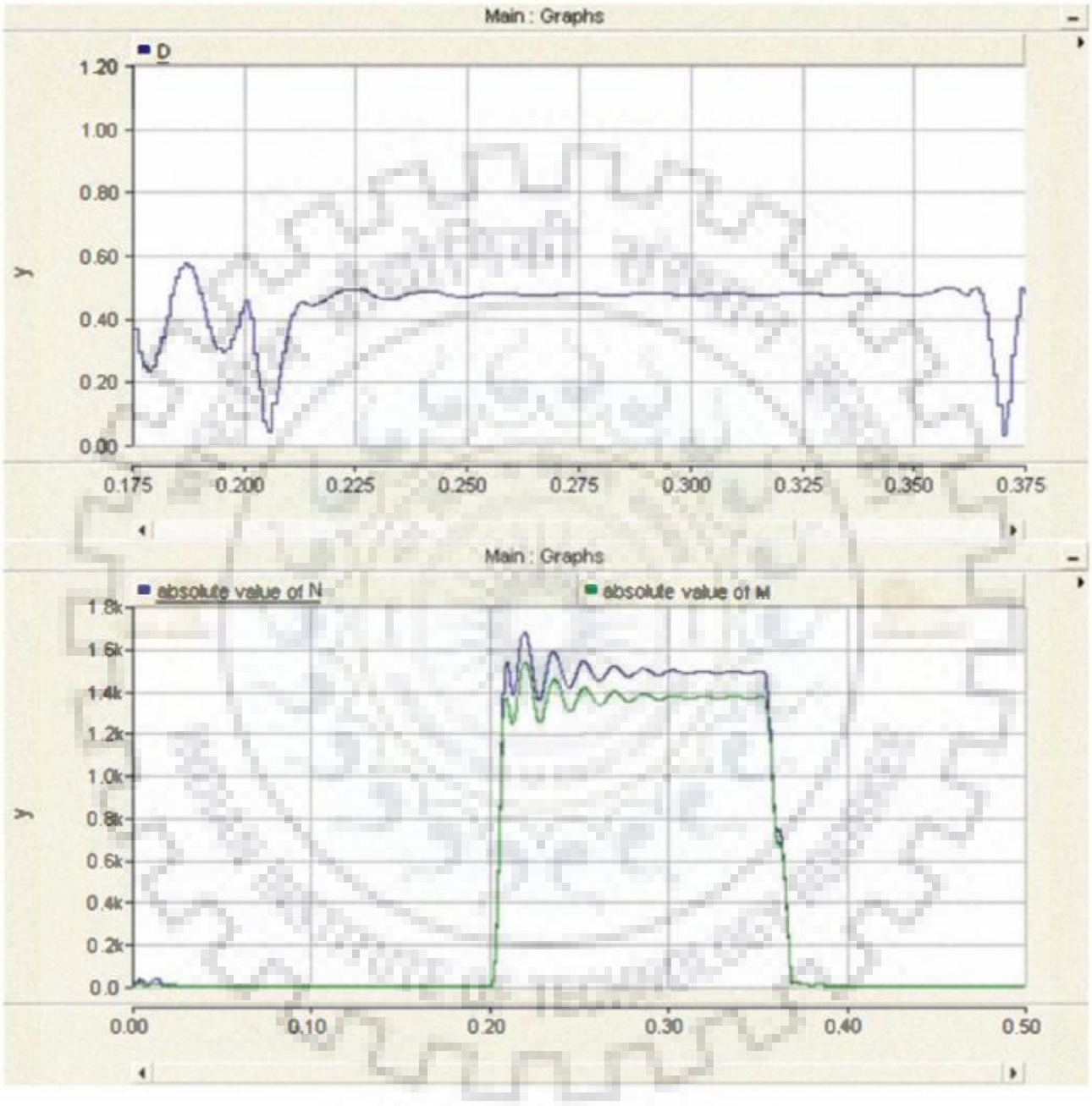

Fig 5.11 : Single phase fault location with D = 0.5

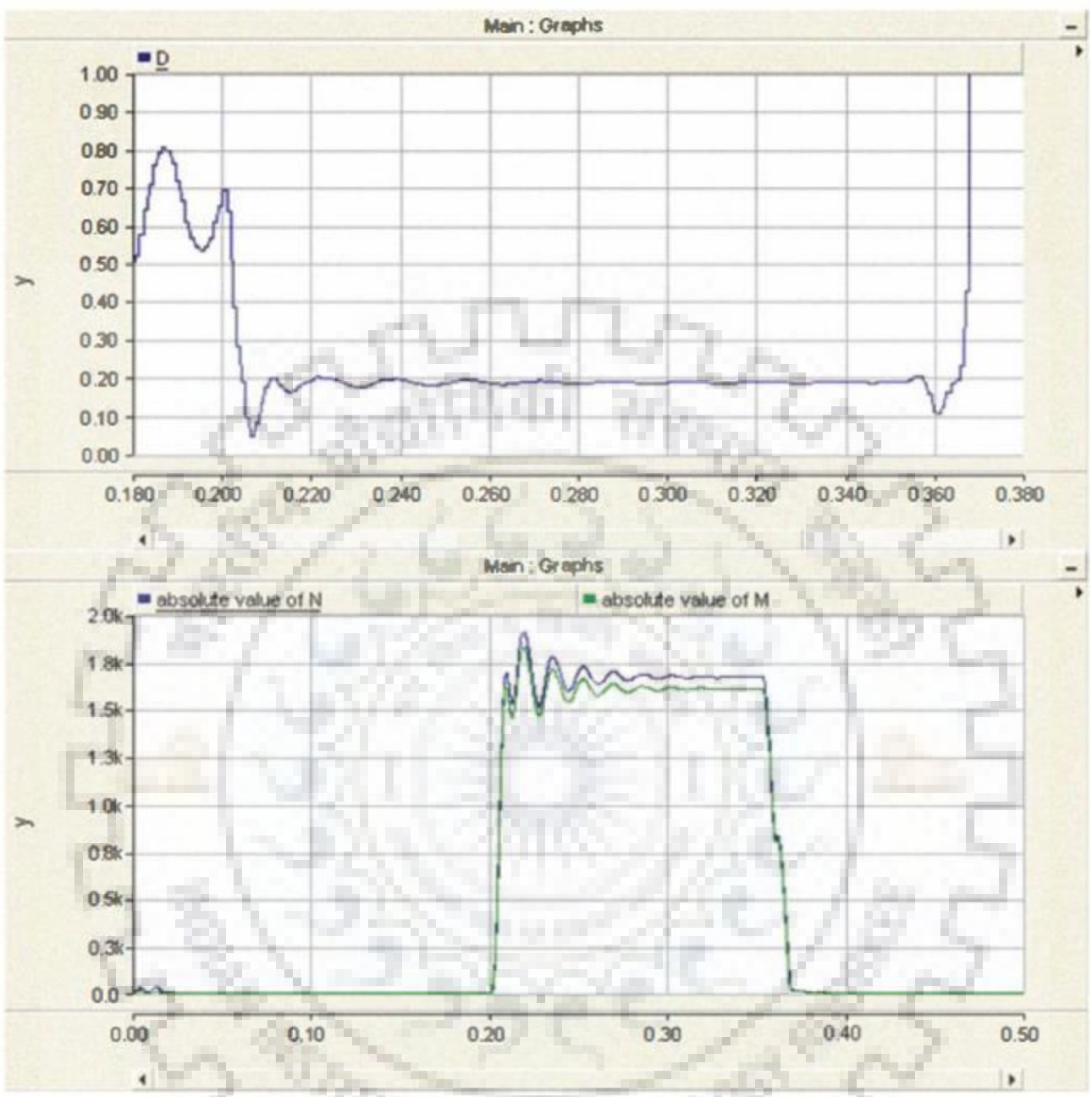

Fig 5.12 : Single phase fault location with D = 0.2

According to the plots, it is obvious that there are some oscillations of the absoulte values of M and N. Here, conventional DFT is used to extract the fundamental components of the voltage and current.

5.5 Estimation of fault location location on UHV transmission line using synchronised PMU measurement

The overall diagram of the fault locator for UHV transmission sysstem using PMU measurments is shown in Appendix A . The phasor measurement units are installed at both ends (sending end S and receiving end R) of the transmission line. The three phase voltages and three phase currents are measured by PMUs located at both ends of line simultaneously. Since the Global Synchronism Clock Generator (GSCG) has been equipped in PMU to provide an extremely accurate and reliable external reference clock signal, it can guarantee sampling synchronization to an accuracy of better than 1 micro sec. The EMTP simulated on 765 kV typical of an Indian transmission System. Voltage and current waveforms were considered to be directly taken as the synchronized sampled data (voltages and currents) from substations S and R . A new DFT method is used to extract close-in fundamental phasors .

5.5.1 Computation of fault detection / location index

The index using the synchronized voltage and current samples at both ends of a transmission line to calculate the location of the fault is presented in this section. Consider an un-faulted single-phase (two-conductors in free space) transmission line shown in Fig. 2. Under sinusoidal steady state condition both voltage and current measured at a distance x km away from receiving end obey two linear differential equations

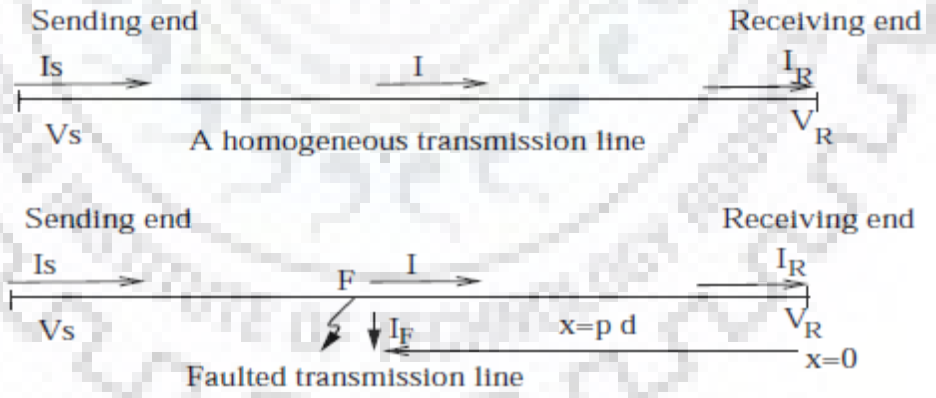

Fig. 5.13 : Transmission line under pre-fault and during fault conditions

$$\frac{dV(x)}{dx} = (R + j\,\omega\, L) \qquad (1)$$

$$\frac{dI(x)}{dx} = (G + j\,\omega\, C) \qquad (2)$$

Solving for equations (1) and (2) by using boundry condition, we get

$$V(x) = \frac{(V_R + I_R Z_C)e^{\gamma x}}{2} + \frac{(V_R - I_R Z_C)e^{-\gamma x}}{2} \quad (3)$$

$$I(x) = \frac{(V_R + I_R Z_C)e^{\gamma x}}{2Z_C} + \frac{(V_R - I_R Z_C)e^{-\gamma x}}{2Z_C} \quad (4)$$

Where x is the distance measured from receiving end

$$V(x) = \frac{(V_S - I_S Z_C)e^{\gamma x}}{2} + \frac{(V_S + I_S Z_C)e^{-\gamma x}}{2} \quad (5)$$

$$I(x) = \frac{(V_S - I_S Z_C)e^{\gamma x}}{2Z_C} + \frac{(V_S + I_S Z_C)e^{-\gamma x}}{2Z_C} \quad (6)$$

Where x is the distance measured from sending end

$$\text{where } Z_C = \sqrt{(R + j\omega L)/(G + j\omega C)}$$
$$\text{and } \gamma = \sqrt{(R + j\omega L)(G + j\omega C)}$$

In case of a fault occurrence at the point *F* which is *x* = *pd* km away from receiving end R on a transmission line S-R shown in Fig. 5.. *d* is the total length of the transmission line, and *p* is the per unit distance from receiving end to the fault and is also used as a fault detection/location index. When fault occurred at the point F, the transmission line is thus divided into two homogeneous parts. Each section acts as independent transmission line. Then the voltage V_F at the point F using both ends boundary conditions is given by

$$V_F(x) = \frac{(V_R + I_R Z_C)e^{\gamma pd}}{2} + \frac{(V_R - I_R Z_C)e^{-\gamma pd}}{2} \quad (7)$$

$$V_F(x) = \frac{(V_S - I_S Z_C)e^{\gamma(1-p)d}}{2} + \frac{(V_S + I_S Z_C)e^{-\gamma(1-p)d}}{2} \quad (8)$$

Eq. (7) and (8) gives the voltage at faulted point *F* in terms of post-fault receiving end and sending end measurements. From equations (7) and (8) fault detection index *p* is obtained as

$$P = \frac{\ln(\frac{Num}{Den})}{2\gamma d} \quad (9)$$

Where

$$Num = (V_R - I_R Z_C) - (V_S - I_S Z_C)\, e^{\gamma d} \quad (10)$$

$$Den = (V_S + I_S Z_C) - (V_R + I_R Z_C)\, e^{\gamma d} \quad (11)$$

Since no assumptions are for deriving index *p*, it is very robust and hardly effected by the variation of source impedance loading change, fault impedance fault inception angle and fault type. Simulations have shown that the proposed index can provide accurate fault location. Absolute values of *Num* and *Den* can be used for fault detector. Pre-fault absolute *Num* and *Den* are equal to zero and during fault abruptly deviated.

5.5.2 Simulation results

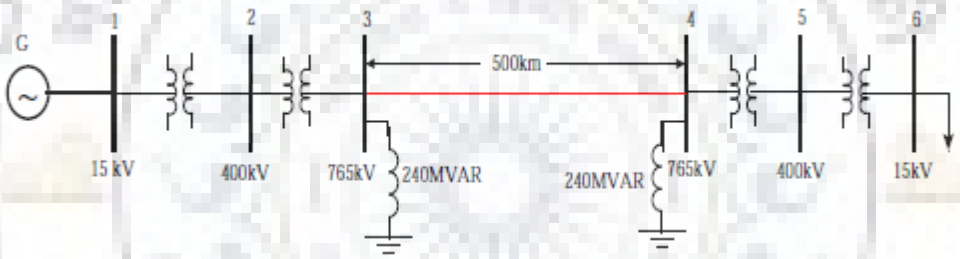

Fig. 5.14 : Test system for 765 kv

The test system considered for studies is a 765kV typical transmission system. Equivalent system diagram is shown in Fig. 5.12 Sending end bus 3 is bus and Receiving end bus is bus 4 . Initially the system is assumed to be operating in steady state balanced condition and delivering a load of 500 MW and 200MVAR. The prefault receiving end quantities are: 4000 MVA, 765 kV. The initial voltages at the buses are obtained from AC load flow solution. The generator side the source strength considered to be 5000 MVA and load side source strength is considered to be 4000 MVA. Faults simulated at ficticious bus 7 at variable distances (p varying from 0.2 to 0.8) from the recienving end bus 4. Results for selected few cases are presented here. The faults for these cases assumed to occur at 0.040 sec. Fault resistance *RF* is varied from 5.852 (0.001 p.u) to 585.2 (0.1 p.u) All currents and voltages are expessed in per unit values on following base values : Base MVA=100 MVA, Base kV=765kV .

Fault current in line 3-7 for 3ph-g fault at a distance (p=0.8) of 400km from sending end is shown in Fig.5.13 The fault is created at 0.4 sec. Fig. 5.14 and Fig. 5.15 shows the current phasor magnitude using conventional DFT and modified DFT respectively.

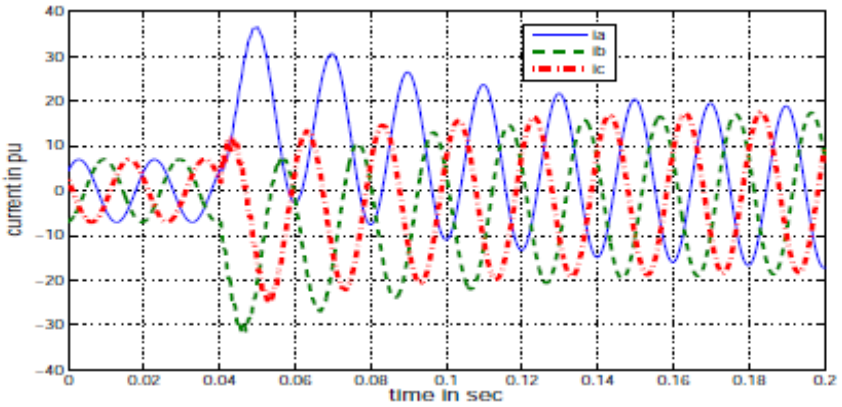

Fig. 5.15. Fault current in line 3-7 for 3ph-g fault for p=0.8 for fault at 0.4sec

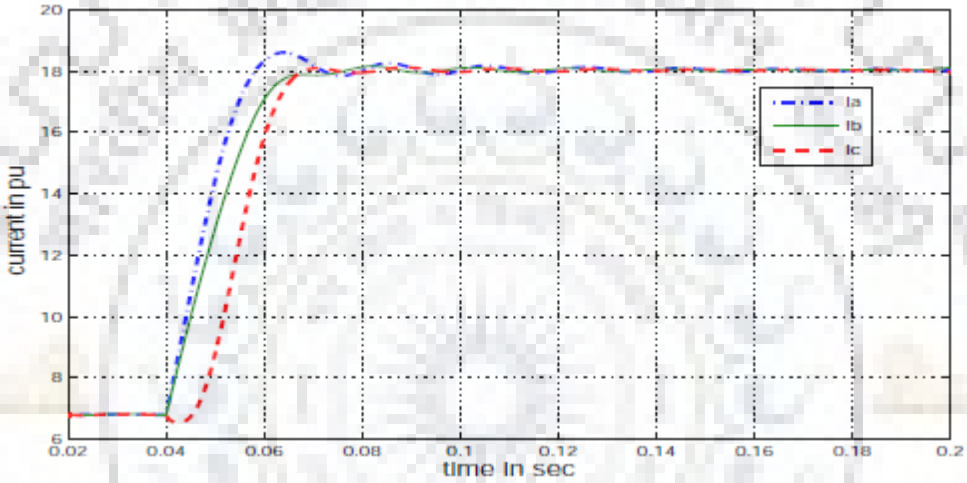

Fig. 5.16. Current phasor for 3ph-g fault for p=0.8 using DFT(0.40sec)

Fault current in line 3-7 for 3ph-g fault at a distance(p=0.8) of 100km from Substation R. is shown in Fig.5.16. The fault is created at 0.45 sec. Fig. 5.17 and Fig.5.18 shows the current phasor magnitude using conventional DFT and modified DFT respectively. The results shows that the new DFT method give the phasors accurately with less oscillations in phasors.

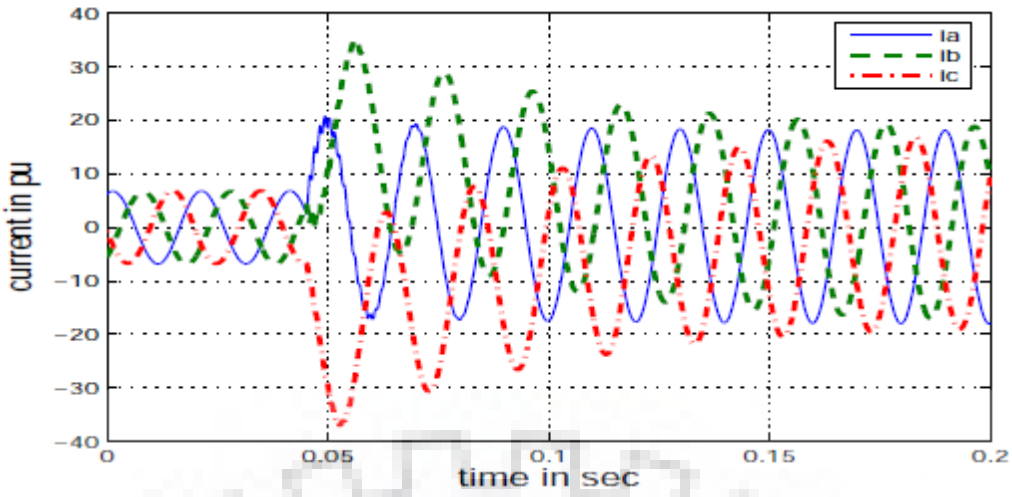

Fig. 5.17. Fault current in line 3-7 for 3ph-g fault for p=0.8 for fault at 0.45sec

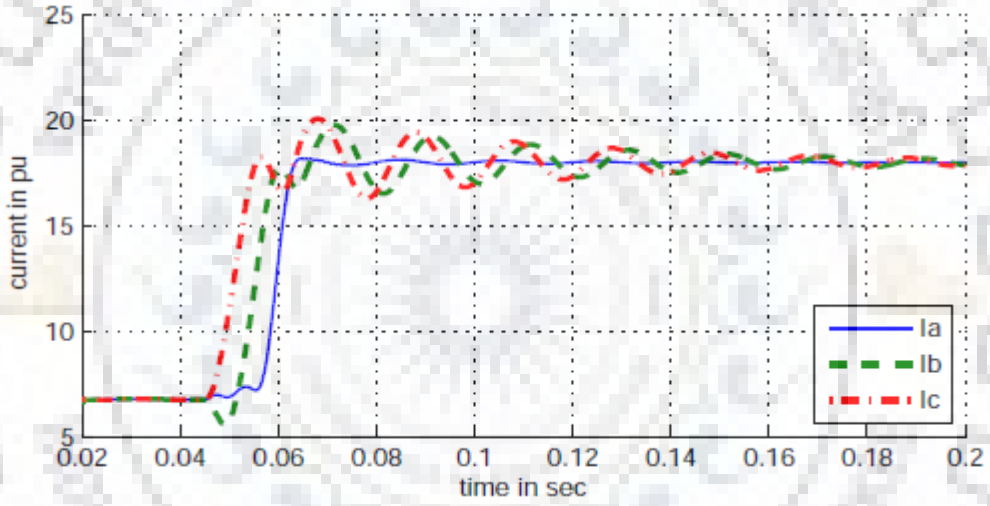

Fig.5.18 . Current phasor for 3ph-g fault for p=0.8 using DFT(0.45sec)

5.5.3 Fault detection and location of 3 ph-g fault

The current and voltage signals at sending end bus (bus 3) located at substation S are shown in Fig 5. 19 and Fig 5.20 when 3ph-g fault occured at a distance of 100km from receiving end (bus4) at substation R at time 0.4 sec and fault resistance is 5.85. The caclulated fault detection indices *Num* and *Den* are shown in Fig 5.22 and Fig 5.23 and the fault location index is shown in Fig 5.21. From the Fig 5.21, Fig 5.22 and Fig. 5.23 it can be observed that the fault detection indices *Num* and *Den* are almost zero before fault (0.04 sec) and *p* has no meaning before fault. when the fault occured (after 0.04 sec the fault detection indices *Num* and *Den* are abruptly deviating from zero for faulted phases and *p* converges to 0.2001.

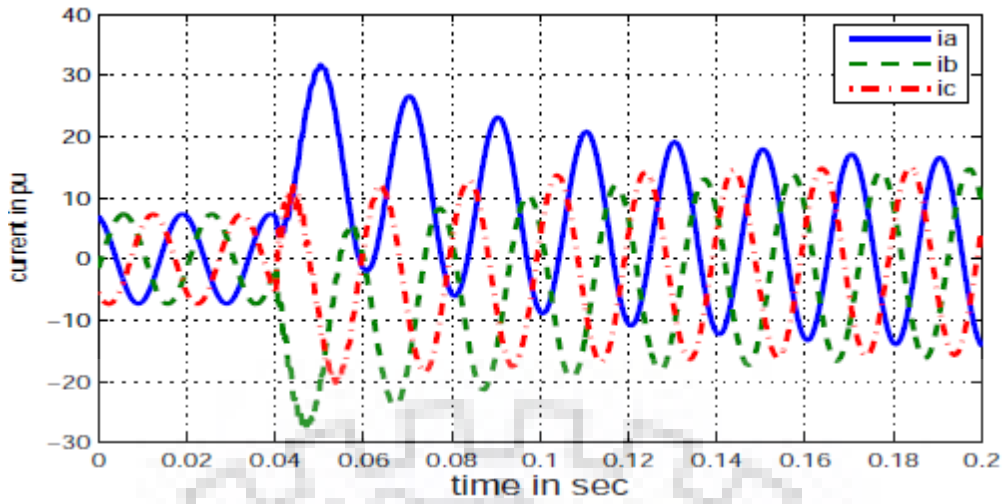

Fig.5.19 : Fault current in line 3-7 for 3ph-g fault (100km from R)

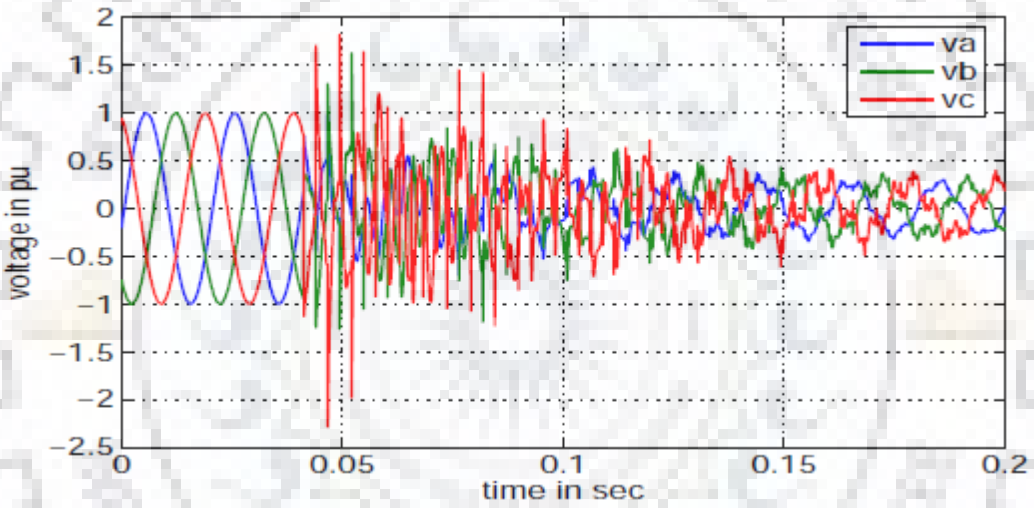

Fig.5.20 : Voltage at bus 3 for 3ph-g fault (100km from R)

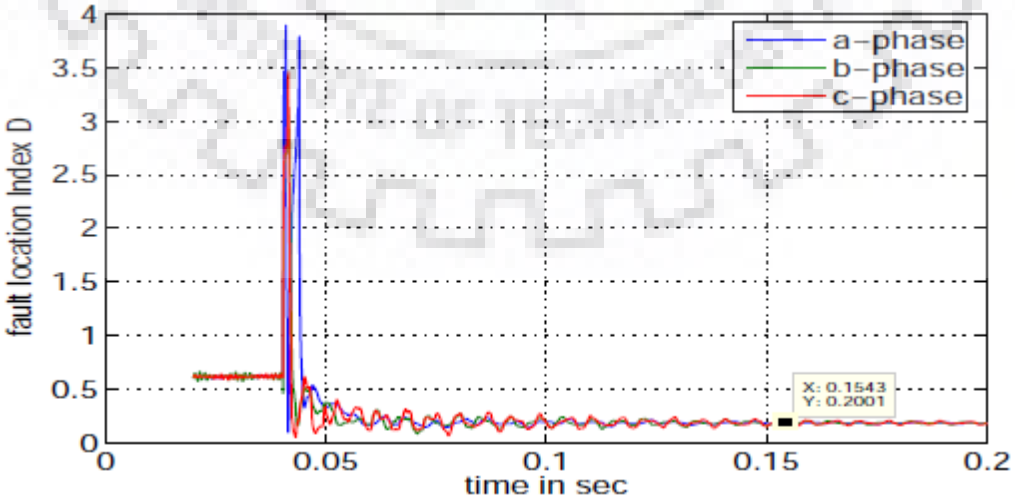

Fig 5.21 : Fault location index p for 3ph-g fault (100km from R)

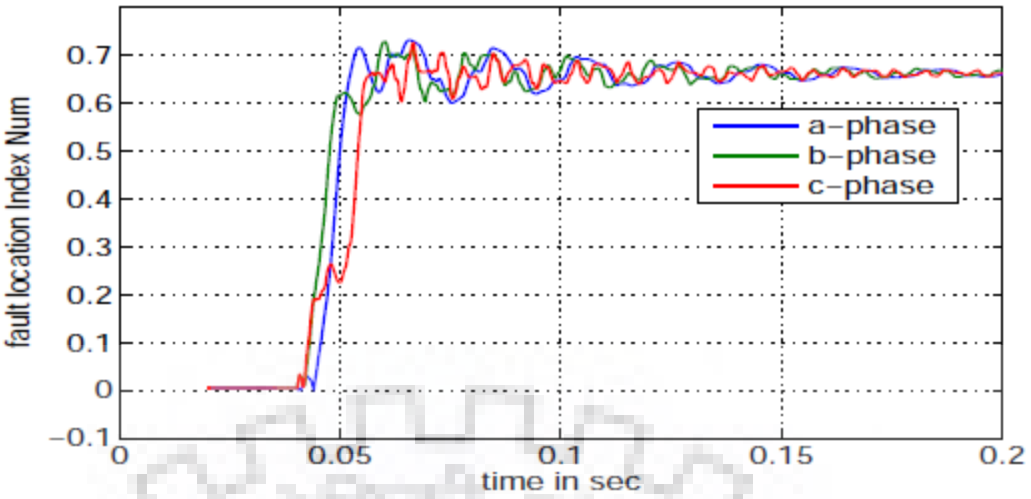

Fig.5.22 : Fault detection index *Num* for 3ph-g fault (100km from R)

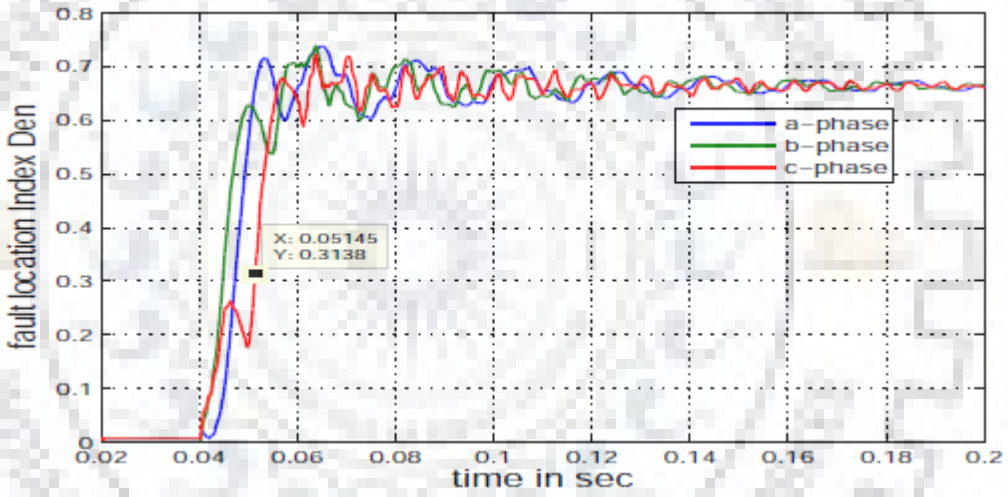

Fig 5.23 : Fault detection index *Den* for 3ph-g fault (100km from R)

CHAPTER 6

PMU APPLICATION IN IDENTIFYING A POWER SWING

In this section we aims to identify a power swing in the power system network as stable or unstable and based on that block or unblock the Zone-3 of distance relays as desired. Determination of the type of swing is carried out by analysing an equivalent single machine infinite bus system, particularly concentrating on the first zero crossing (FZC) of the speed of the machine. The equations for this algorithm are developed using the local measurements (obtained from a PMU or CT/PT) at a relay location along with the power-angle characteristics equations.

6.1 Methodology

The working of the algorithm has been explained using a 3-bus, 345 kV test power system in which a three phase fault is created on transmission line 1-2 (as shown in Figure 6.1).

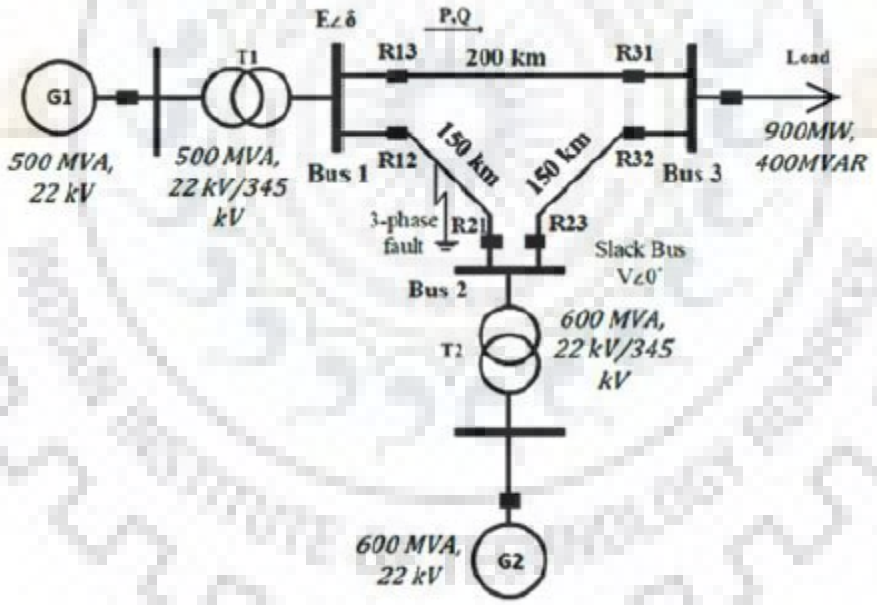

Fig 6.1 : Three bus test system

Under fault condition, the values of different electrical quantities as seen by the relay R13 (measured by a PMU located near the relay) can be used to represent the whole test system in the form of a single machine infinite bus (SMIB) equivalent system as depicted in Figure 6.2.

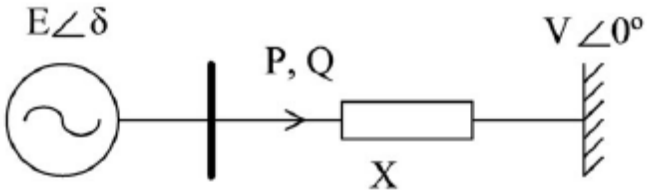

Fig 6.2 : SMIB Model

Now, in order to analyze the SMIB system, the values of bus voltage (E∟δ), reactive power (Q) and active power (P) must be obtained. These values are measured at bus-1 (as seen by relay R13). V is measured at bus-2. Also, there are two unknown parameters of the SMIB system, the voltage angle (δ) and the equivalent reactance (X), which can be determined as follows.

The power flow equations for a simple SMIB system is given by

$$P = \frac{EV}{X} \sin \delta \qquad (6.1)$$

$$Q = \frac{E^2}{X} - \frac{EV}{X} \cos \delta \qquad (6.2)$$

Where,

P is active power

Q is reactive power

E is magnitude of bus-1 voltage

V is magnitude of bus-2 voltage

X is equivalent resistance

δ is angle difference between bus-1 and bus-2

Elimination of δ from eqns. (6.1) and (6.2) leads to

$$\left(\frac{PX}{EV}\right)^2 + \left(\frac{E^2 - QX}{EV}\right)^2 = 1$$

In order to solve for X, the following equation is obtained

$$(P^2+Q^2)X^2-2E^2QX+E^4-E^2V^2=0$$

After having obtained all the parameters of the SMIB system, the next step in the algorithm involves calculating the speed of the _ctitious synchronous machine of the SMIB system as shown in Figure 6.2 during a power swing. The speed of the representative machine is obtained from eqns. (6.1) and (6.2). By differentiating (6.1), the following equation can be obtained.

$$\frac{dP}{dt}=\left(\frac{EV}{X}\right)\cos\delta\left(\frac{d\delta}{dt}\right)$$

The expression for cos δ can be derived from eqn .(6.2) as

$$\cos\delta=\left(\frac{E^2-QX}{EV}\right)$$

and also dδ/dt can be written as ω_r, where ω_r is relative speed of the fictitious synchronous machine.

$$\omega_r=\frac{\frac{dP}{dt}}{\left(\frac{E^2-QX}{X}\right)}$$

Substituting eqn . (6.6) and ωr in eqn. (6.5), the following is obtained

The expression for $\frac{dP}{dt}$ can be approximated as ,

$$\frac{dP}{dt}=\frac{\Delta P}{\Delta T} \qquad (5.8)$$

And also

$$\frac{\Delta P}{\Delta t}=\frac{P_t-P_{t-1}}{\Delta t}$$

where ΔP and Δt (time step) are values obtained from MATLAB simulation. Substituting eqn.(6.9) in eqn.(6.8) and then in eqn.(6.7), finally the following equation is obtained :

$$\omega_r = \frac{\left(\frac{P_t - P_{t-1}}{\Delta t}\right)}{\left(\frac{E^2 - QX}{X}\right)}$$

6.2 DETERMINATION OF TYPE OF POWER SWING

ω_r as obtained above is plotted against time to see if the relative speed of the SMIB generator crosses zero value or not. This zero crossing of the relative speed will help to identify the type of swing in the power system. Hence, the power swing can be identified to be a stable one if ω_r crosses zero value, otherwise it is an unstable swing.

Zero crossing implies that the speed of the fictitious generator of the equivalent SMIB system reaches the synchronous value before accelerating/decelerating again. Whereas the event of non-zero crossing implies that the machine doesn't attain the synchronous value before accelerating again. The proposed algorithm utilises this feature to decide the nature of the power swing. A simple diagrammatic representation of the variation of the relative speed of the machine is shown in Figure 6.3.

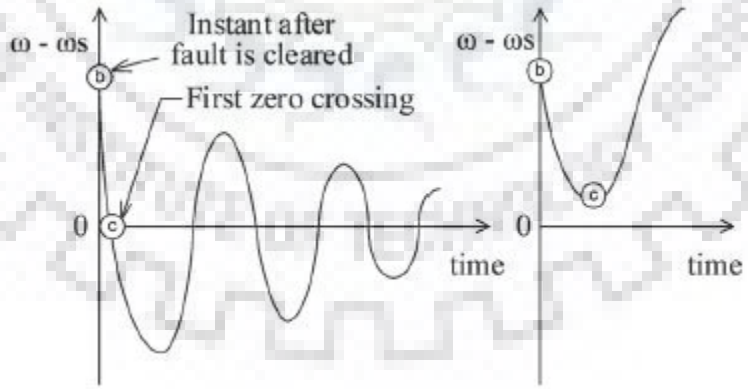

Figure 6.3: Speed variation of SMIB machine during stable and unstable power swings

6.3 SIMULATION STUDIES ON 3 –BUS SYSTEM

The simulations to implement the algorithm have been carried out on a 3-bus, 345 Kv test system. A 3-phase fault is created at a distance of 50 km from bus-1 on the transmission line joining buses 1 and 2 as shown in Figure 6.1. The instant at which the fault is applied is 2 s and the duration of the fault is 0.1 s. The plot of variation of the relative speed of the fictitious machine with respect to time as derived from the algorithm is depicted in Figure 6.4. From the figure, it can be observed that the firrst zero crossing occurs immediately after the fault is cleared thus indicating a stable power swing.

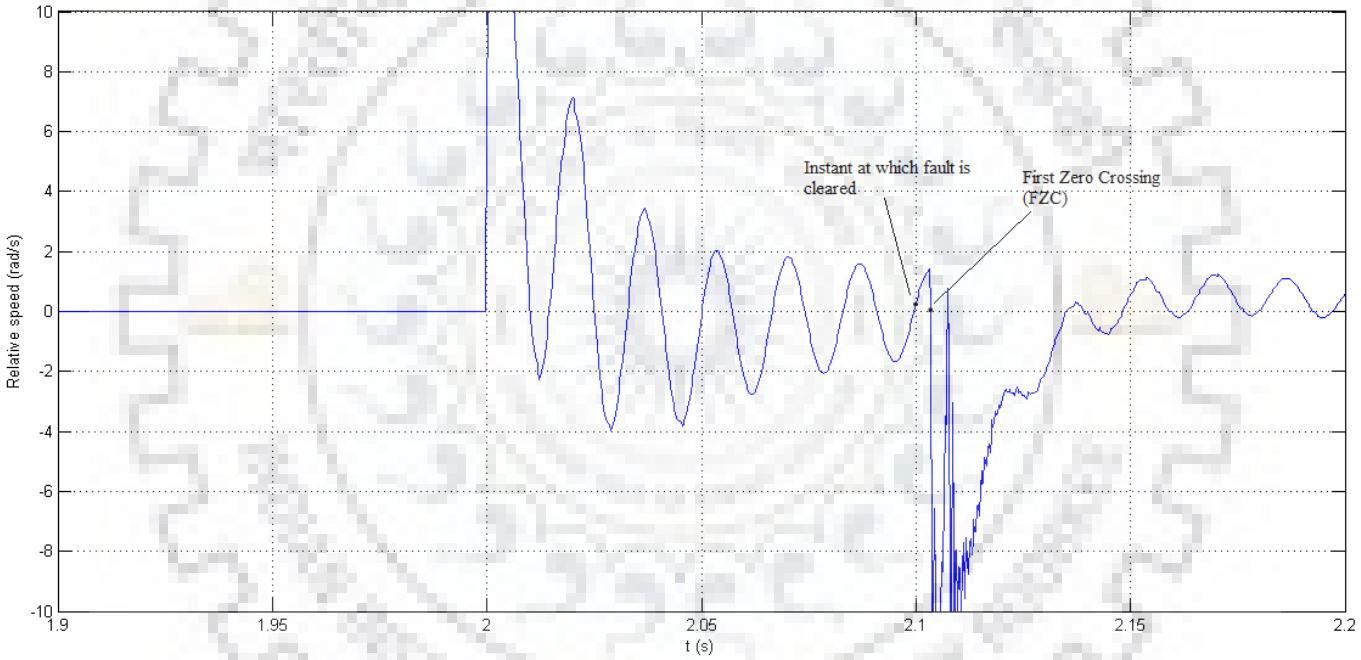

Figure 6.4: Relative speed of SMIB machine obtained in accordance with the proposed algorithm

An unstable swing is generated in the test system at t = 2 s for a duration of 0.2 s. The variation of ω_r of the machine with respect to time is shown in Figure 5.5. It can be observed from the figure that the relative speed of the _ctitious machine doesn't cross the zero line immediately. However, when the unstable swing becomes stable, then it is observed that the relative speed of the generator crosses the zero line.

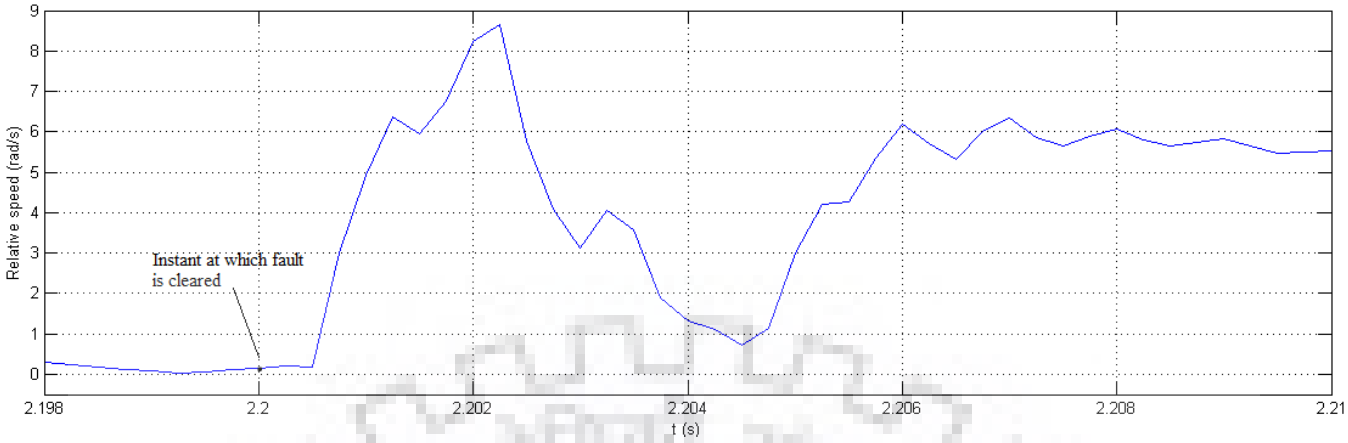

Figure 6.5 : Relative speed of SMIB machine obtained in accordance with the proposed algorithm

CHAPTER 7

DISCUSSION AND CONCLUSION

The dissertation report addresses the main reasons for execution of WAMPAC systems. In the initial part of the report we have discussed the need of WAMS, its architecture and its benefits . The most important unit of WAMS is PMU. We have discussed PMU in detail.

A typical WAMPAC structural design is presented with its main building blocks (PMUs). The structural design depends on unambiguous system needs, its topology, creation profile, and the quality of the communication infrastructure. The report also provides a general idea of the main WAMPAC applications and demonstrates some applications that is, dynamic recording, real time system state determination, phase angle and disturbance propagation monitoring, estimation of load model parameters, as well as protection and control related applications.

We have dicussed the application on PMU in fault location techniques.With the use of PMU the sampling rate required for fault location in much lesser due to its fast operation.So it is advantageous to use PMU in fault location techniques.

We have also discussed that PMU data can also be used in identifying whether a power swing created after a disturbance is stable or unstable by analyzing an equivalent SMIB system especially focusing on the variation of the relative speed of the equivalent synchronous machine with respect to time in order to obtain the first zero crossing instant of the relative speed.

REFRENCES

[1]Y. Liu, L. Zhan, D. Zhou, J. Guo, Y. Lei, G. Kou, W. Yao, J. Chai, and Y. Liu "Wide-Area-Measurement System Development at the Distribution Level: An FNET/GridEye Example ", IEEE Transaction On Power Delivery, VOL. 31, NO. 2, pp. 721-731, APRIL 2016 .

[2] G. A. Taylor, I. Pisica, P. Ashton,M. Golshani," Implementation of Wide Area Monitoring Systems and Laboratory-based Deployment of PMUs ", IEEE paper.

[3] V.Terzia ,G.Valverde,D. Cai,J.Fitch,p.Regulaski "Wide-Area Monitoring, Protection, and Control of Future Electric Power Networks", IEEE paper.

[4] B.Pinte, M.Quinlan, K.Reinhard "Low Voltage Micro-Phasor Measurement Unit (μPMU) ", IEEE paper.

[5] Y.Liu, S. You, Y. Cui ,H.Liu, "A Distribution Level Wide Area Monitoring System for the Electric Power Grid—FNET/GridEye",IEEE Paper,March 2017.

[6] R.B. Bobba, J. Dagle, E. Heine, H. Khurana, W.H. Sanders, P. Sauer, T. Yardley, "Enhancing Grid Measurements: Wide Area Measurement Systems, NASPInet, and Security," Power and Energy Magazine, IEEE , vol. 10, no. 1, pp. 67-73, Jan-Feb 2012.

[7] C. Martinez, M. Parashar, J. Dyer, and J. Coroas, ''Phasor Data Requirements for Real Time Wide-Area Monitoring, Control and Protection Application,'' EIPP White Paper, Jan. 26, 2005, p.8 .

[8] Waheed Ur Rahman, Muhammad Ali, Amjad Ullah, Hafeez Ur Rahman, Majid Iqbal, Haseeb Ahmad, Adnan Zeb, Zeeshan Ali, M. Ahsan Shahzad, Beenish Taj, " Advancement in Wide Area Monitoring Protection and Control Using PMU's Model in MATLAB/SIMULINK",Smart grid and renewable energy, vol.3.pp.294-307.

[9] Jim Y Cai , Zhenyu Huang, John Hauer ,Ken Martin," Current Status and Experience of WAMS Implementation in North America",IEEE paper,2005.

[10] X. Xie,Y. Xin,J. Xaio,Jintago Wu,"WAMS application in Chinese power system",IEEE Power and Energy Magazine,2006.

[11] Moustafa Chenine, Member, IEEE, Luigi Vanfretti, Member, IEEE, Sebastian Bengtsson, and Lars Nordstrom, Member, IEEE," Implementation of an Experimental Wide-Area Monitoring Platform for Development of Synchronized Phasor Measurement Applications",IEEE paper.

[12] Bipul Luitel, Ganesh K. Venayagamoorthy ,and Cameron E. Johnson, "Enhanced Wide area monitoring system",IEEE paper.

[13] G.B.Ancell and N. C.Pahalawaththa, "Maximumu likelihood estimation of fault location on transmission line using travelling waves," IEEE Trans. Power Del., vol. 9, no. 2, pp. 680-689, April 1994.

[14] M.H.Bollen, "Traveling-wave-based protection of double-circuit lines,"Proc. Inst. Elect. Eng., pt. C" vol. 140, no. I, pp. 37-47, Jan 1993.

[16] F. H.Magnago and A. Abur, "Fault location using wavelets," IEEE Trans. Power Del., vol. 13, no. 4, pp. 1475-1480, Oct. 1998.

[17] D. Spoor and J. G. Zhu, "Improved single-ended traveling-wave faultlocation algorithm based on experience with conventional substation transducers," IEEE Trans. Power Del., vol. 21, no. 3, pp. 1714-1720, July 2006.

[18] T.Takagi, Y.Yamakoshi, M.Yamaura, R.Kondow, and T.M.atsushima, "Development of a new type fault locator using the one-terminal voltage and current data," IEEE Trans. Power App. Syst., vol. PAS-101, no. 8, pp. 2892-2898, August 1982.

[19] T.Takagi, Y.Yamakoshi, J.Baba, K.Uemura, and T.Sakaguchi, "A new alogrithm of an accurate fault location for ehv/uhv transmission line: Part i-fourier transformation method," IEEE Trans. Power App. Syst., vol. PAS-IOO, no. 3, pp. 1316-1323, March 1981.

[20] L. Eriksson, M. M. Saha, and G. D. Rockefeller, “An accurate fault locator with compensation for apparent reactance in the fault resistance resulting from remote-end infeed,” IEEE Trans. Power App. Syst, vol. PAS-104, no. 1, pp. 424–436, Feb. 1985.

[21] L. Jie, S. Elangovan, and J. B. X. Devotta, “Adaptive travelling wave protection algorithm using two correlation functions,” IEEE Transactions on Power Delivery, vol. 14, no. 1, Jan. 1999

[22] Phadke A. G. and Thorp J.S., “ Synchronized Phasor Measurement and Their Applications”, Springer, USA, 2008

[23] Phadke A. G., Thorp J.S. and De La Ree Jaime, “Synchronized Phasor Measurement Applications in Power Systems”, IEEE Transactions On Smart Grid, Vol. 1, No. 1, June 2010

[24]Adamiak Mark, Premerlani William and KasztennyBodgan, “Synchrophasors: Definition, Measurement, and Application”, General Electric Co., Global Research

[25] IEEE Std C37.118-2005 for Synchrophasors for Power Systems.

[26] Dotta Daniel and Chow Joe H., “A MATLAB-based PMU Simulator”, IEEE Fellow.

[27] G. K. Purushothama, A. Narendranath, D. Thukaram, and K. Parthasarathy, “Ann applications in fault locators,” *Electric Power and Energy Systems*, vol. 23, pp. 491–506, 2001.

[28] D. Novosel, D. G. Hart, E. Udren, and J. Garitty, “Unsynchronized two terminal fault location estimation,” *IEEE Trans. Power Del*, vol. 11, no. 1, pp. 130–138, Jan. 1996.

[29] A. Jiang, J.-Z. Yang, Y.-H. Lin, C.-W. Liu, and C. Ma, “An adaptive pmu based fault detection/location technique for transmission lines-i. theory and algorithms,” *IEEE Trans. Power Del*, vol. 15, no. 2, pp. 486–493, Apr. 2000.

[30] Y.-S. Cho, C.-K. Le, G. Jang, and H. J. Lee, “An innovative decaying dc component estimation algorithm for digital relaying,” *IEEE Transactions on Power Delivery*, vol. 24, no. 1, pp. 73–78, Jan. 2009.

[31] H. W. Dommel, *Electromagnetic Transients Program Theory Book*. BPA, Jul. 1994.

[32] A. Phadke and J. Thorp, *Computer Relaying For Power Systems*. John Wiley & Sons, 1988.

[33] D. Thukaram, S. R. Kolla, K. Ravishankar, and A. Rajendra Kumar, “Switching and fault transient analysis of 765 kv transmission systems,”*Third International Conference on Power Systems, Kharagpur, INDIA*, no. 122, Dec. 2009.

[34] T. S. Sidhu, X. Zhang, F. Albasri, and M. S. Sachdev, “Discretefouriertransform-based technique for removal of decaying dc offset from phasor estimates,” *Proc. Inst. Elect. Eng., Gen.., Transm. Distrib*, vol. 150, no. 6, pp. 745–752, Nov. 2003.

[35] Z. Qingchao, Z. Yao, S. Wennan, Y. Yixin, and W Zhigang, "Fault location of two-parallel transmission line for non-earth fault using oneterminal data," IEEE Trans. Power Del., vol. 14, no. 3, pp. 863-867, July 1999.

[36] D. A.Tziouvaras, J. Roberts, and G. Benmouyal, "New multi-ended fault location design for two- or three-termianl lines," lEE Developments in Power System Protection, no. 479, pp. 395-398, 2001.

[37] S.-H. Kang, Y.-J. Ahn, Y.-C. Kang, and S.-R. Nam, "A fault location algorithm based on circuit analysis for untransposed parallel transmission lines," IEEE Trans. Power Del., vol. 24, no. 4, pp. 1850-1856, October 2009.

[38]J.-A. Jiang, J.-Z. Yang, Y.-H. Lin, C.-W Liu, and Jih-Chen, "An adaptive pmu based fault detection/location technique for transmission lines-part i: Theory and aligorithms," IEEE Trans. Power Del., vol. 15, no. 2, pp. 486-493, April 2000.

[39]J.-A. Jiang, Y.-H. Lin, J.-Z. Yang, T.-M. Too, and c.-w Liu, "An adaptive pmu based fault detection/location technique for transmission lines-part ii: Pmu implementation and performance evaluation," IEEE Trans. Power Del., vol. 15, no. 4, pp. 1136-1146, October 2000.

[40]C.-S. Yu, C.-W Liu, S.-L. Yu, and J.-A. Jiang, "A new pmu-based fault location algorithm for series compensated lines," IEEE Trans. Power Del., vol. 17, no. I, pp. 33-46, January 2002.

Appendices

APPENDIX A

Fault locator algorithm using PMU measurements

The three phase voltages and three phase currents are measured by PMUs located at both ends of line simultaneously. Since the Global Synchronism Clock Generator (GSCG) has been equipped in PMU to provide an extremely accurate and reliable external reference clock signal, it can guarantee sampling synchronization to an accuracy of better than 1 micro sec. . Voltage and current waveforms were considered to be directly taken as the synchronized sampled data (voltages and currents) from substations Anpara and Unnao. A new DFT method is used to extract close in fundamental phasors.

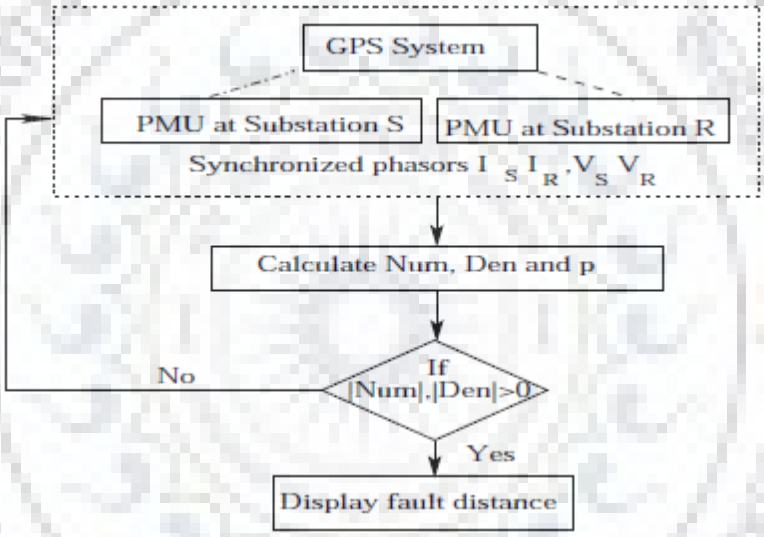

Fig. 1 : Fault locator for using PMU measurement

APPENDIX B

Parameters of transmission line used as test system for fault location

B .1 Parameters of three phase transmission line used for negative sequence impedence method :

Data of two sources And transmission line :

Data of source at sending end S	Mag.(AC,L-L, RMS) :230 KV Frequency : 50 Hz Phase shift : 0 deg
Data of source at receiving end R	Mag.(AC,L-L, RMS) :230 KV Frequency : 50 Hz Phase shift : 20 deg

	R	**X**
Positive sequence	12.868	182.79
Negative sequence	12.868	182.79
Zero sequence	130.735	477.53
Lenghth of transmission line = 360 km		

B.2 Parameters of single phase transmission line used in distributed transmission line model :

Parameters of two sources And transmission line :

Sending end source	Mag.:(AC,L-G,RMS) : 230KV Frequency: 50 HZ Phase shift : 0 degree
Receiving end source	Mag.:(AC,L-G,RMS) : 230KV Frequency: 50 HZ Phase shift : 20 degree

R (Ω/km)	L (H/km)	C (F/km)	G (Ωkm)^ -1
0.1236	0.0021	0.1 * 10 ^ -7	7.49 *10 ^ -7
Length of transmission line = 180 km			